Check for updates

European Journal of Soil Science

WILEY

European Journal of Soil Science

RESEARCH ARTICLE OPEN ACCESS

Pedotransfer Functions Versus Model Structure: What Drives Variance in Agro-Hydrological Model Results?

Maria Eliza Turek[1,2] | Johannes Wilhelmus Maria Pullens[3] | Katharina Hildegard Elisabeth Meurer[4] | Edberto Moura Lima[5] | Bano Mehdi-Schulz[5] | Annelie Holzkämper[1,2]

[1]Agroscope, Zürich, Switzerland | [2]Oeschger Centre for Climate Change Research, University of Bern, Bern, Switzerland | [3]Department of Agroecology, Aarhus University, Tjele, Denmark | [4]Department of Soil and Environment, Swedish University of Agricultural Sciences – SLU, Uppsala, Sweden | [5]University of Natural Resources and Life Sciences, Vienna (BOKU), Institute of Hydrology and Water Management, Vienna, Austria

Correspondence: Maria Eliza Turek (mariaeliza.turek@agroscope.admin.ch)

Received: 3 October 2024 | **Revised:** 21 January 2025 | **Accepted:** 27 February 2025

Funding: This study was developed in the framework of the project SoilX (Soil management to mitigate climate change-related precipitation eXtremes), which is part of the European Joint Program for SOIL "Towards climate smart sustainable management of agricultural soils" (EJP SOIL) funded by the European Union Horizon 2020 research and innovation program (grant agreement no. 862695).

Keywords: APEX | CANDY | DAISY | evapotranspiration | lysimeter | model ensemble | seepage | soil water | SWAP | yield

ABSTRACT

Pedotransfer functions (PTFs) are widely used empirical relationships to estimate soil hydraulic parameters. PTFs are usually derived from point soil samples analysed in the field or laboratory; thus, they contain uncertainties at different levels (i.e., from sampling and measuring techniques, as well as empirical approaches chosen to quantify relationships). When PTFs are used to parametrize agro-hydrological models, both the choice of PTF and the choice of the model may influence the simulation results. Both sources of variance (PTF choice and model structural differences) were found to be relevant in previous studies, but how they relate to each other has rarely been investigated. In this study, we addressed this research gap by conducting a systematic analysis of the variance in selected agro-hydrological model outputs (i.e., seepage water, soil water content, actual evapotranspiration, transpiration, biomass production) based on an ensemble of 18 PTFs applied to four agro-hydrological models, namely: APEX, CANDY, DAISY and SWAP. The models were calibrated for aboveground biomass and phenology of silage maize and evaluated using data of actual evapotranspiration, seepage water and soil water content obtained from a lysimeter facility in Switzerland. ANOVA-based variance partitioning was applied to attribute variance in model outputs to two uncertainty sources (PTF choice, model choice). Overall, we found that agro-hydrological model structural differences had a larger influence on the variance in model outputs than PTF differences. Further analyses undertaken per model showed that the sensitivity of the simulated outputs to the choice of PTF differed between the models; our results showed that the models integrating the Richards equation (SWAP, DAISY) were more sensitive to the choice of PTF than those using a reservoir cascade approach (APEX, CANDY). Our results also showed that simulated outputs using the mean of a PTF ensemble performed better than when using a single PTF, irrespective of the model and output variable. We therefore recommend using PTF ensembles in agro-hydrological modelling studies. The benefit of using large PTF ensembles is, however, likely to be reduced in larger ensembles of agro-hydrological models, as structural model uncertainties will dominate over PTF uncertainties, according to the four-member model ensemble investigated here.

This is an open access article under the terms of the Creative Commons Attribution License, which permits use, distribution and reproduction in any medium, provided the original work is properly cited.

© 2025 The Author(s). *European Journal of Soil Science* published by John Wiley & Sons Ltd on behalf of British Society of Soil Science.

Summary

- Influences of PTFs on the variance of multi-model simulated outputs are not well understood.
- An ensemble of 4 models and 18 PTFs was employed to analyse variance sources.
- Propagation of uncertainty from a given PTF depends on the choice of model.
- Variance due to model structural differences is mostly higher than due to PTF choice.

1 | Introduction

Agro-hydrological models are commonly applied to cropping systems for evaluating the influence of climate, soil and management drivers on environmental processes involving water fluxes (e.g., transpiration, runoff, leaching of nutrients and pesticides), both at local and regional scales. Depending on the scale of interest, the parameterization of the soil hydraulic parameters (SHP) is carried out using actual observed data or by using estimates from pedotransfer functions (PTFs). PTFs are relationships or knowledge rules used to relate easy-to-measure soil information to other soil properties or variables that are needed to parameterise the soil processes in land surface models (Looy et al. 2017). Using input variables, such as soil texture, bulk density and soil organic carbon, PTFs are commonly applied to predict SHP, relying on databases that are available from field or laboratory measurements. It is thus not surprising that estimates from PTFs are subject to uncertainties (e.g., Stenemo and Jarvis (2007), Deng et al. (2009), Loosvelt et al. (2011), Weber et al. (2024)). Efforts to reduce uncertainties in PTFs are constantly undertaken (Szabó et al. 2021; Zhang et al. 2020; Ding and El-Zein 2024) and the ability of different PTFs to predict soil water content or soil hydraulic conductivity has been tested in various studies (e.g., Nasta et al. (2021)). Furthermore, it has been explored in several modelling studies how the choice of PTF affects simulation results of agro-hydrological studies. For example, Weihermüller et al. (2021) applied HYDRUS-1D in combination with several widely used PTFs to find that PTF choice led to substantial variability in the predicted water fluxes. Similarly, Paschalis et al. (2022) evaluated the responses of the eco-hydrological and terrestrial biosphere model T&C and quantified how uncertainties embedded in using different PTFs propagate to simulated water and carbon fluxes. They found that PTF differences resulted in roughly 10% variation in the simulated leaf area. Other studies have included more than one model in the evaluation of PTF uncertainties to study to which extent specific models are sensitive to PTF choices (e.g., Baroni et al. (2010), Liao et al. (2020)). By considering more than one agro-hydrological model, the uncertainty in the simulated results will contain combined effects of structural model differences (i.e., structural model uncertainty) and uncertainties originating from PTF choice. Model structural differences in agro-hydrological models originate, for example, from different representations of the soil water balance (i.e., Richards'-based versus a reservoir cascade implementation), or the response of plant water stress to different soil water content conditions and its influence on plant transpiration and productivity, as well as the parameterisation of the soil evaporation interaction with surface soil water content. Some studies have addressed both structural model uncertainties and uncertainties resulting from PTF choice. For example, Baroni et al. (2010) used the Richards'-based model SWAP and the reservoir cascade model ALHyMUS with SHPs parameterised using laboratory measurements, field data and PTFs to assess the variability of simulated soil water content and bottom flux in a study in Northern Italy. The findings highlighted that the variability of the simulated water dynamics for different SHP sets was found to often be larger than the difference between model results of the two models using the same SHP set, indicating that model structural differences had a smaller effect on the results as compared to SHP. Beyond soil water dynamics, Liao et al. (2020) assessed model versus SHP parameterisation uncertainties applying two biogeochemical models (DayCent and DeNitrification-DeComposition, DNDC) to simulate soil NO_3^-—N leaching on a tea garden hillslope in Taihu Lake Basin, China. Using an ensemble of 12 PTFs, the authors found that both PTF choice and model structural differences had similar effects on variance in simulated soil NO_3^-—N leaching. The majority of the studies that investigate the effects of PTF uncertainties in agro-hydrological models have only explored sensitivities of model estimates to PTF choices based on single or pairs of models. It is thus not well understood how uncertainties originating from PTF choices compare to model structural uncertainties in larger model ensembles. We addressed this research gap by applying an ensemble of four agro-hydrological models in combination with 18 PTFs to systematically explore how different model structures mediate the influence of PTF parameterisation. Two of the four agro-hydrological models use a reservoir cascade scheme (APEX, CANDY) and therefore were expected to be less sensitive to the PTF choice, while the other two models describe the space–time variation of soil water content based on the Richards equation (DAISY, SWAP). We systematically investigated the effect of PTF choice as compared to model structural differences in selected outputs describing the soil-crop-water dynamics.

2 | Materials and Methods

2.1 | Study Site and Reference Data

The reference data used in this study was obtained from the lysimeter facility of Agroscope Zürich-Reckenholz (Prasuhn et al. 2016). Additional data on averages of flowering days and crop yield was obtained from silage maize variety trials in Zürich-Reckenholz (Baux et al. 2010; Hiltbrunner et al. 2014; 2015; 2016; 2017; 2018; 2019; 2020; 2021; 2022; 2023). The meteorological data was obtained from a MeteoSwiss monitoring station (REH, latitude 47°26′ N, longitude 8°31′ E, altitude 443 m) located near the lysimeters. Our analysis was focused on 2 years with distinct climate patterns. In 2015, the average precipitation during summer (May to September) was 421 mm; therefore, drought conditions were observed. In contrast, 2021 had a total of 609 mm precipitation during the same period and was considered to be a wet year for local conditions (Figure 1). For an extended dataset with data from 2009 to 2022, see Appendix A1.

Data for aboveground biomass, soil water content, actual evapotranspiration (AET), and seepage water were obtained from a

13652389, 2025, 2, Downloaded from https://bsssjournals.onlinelibrary.wiley.com/doi/10.1111/ejss.70088 by Schweizerische Akademie Der, Wiley Online Library on [27/03/2025]. See the Terms and Conditions (https://onlinelibrary.wiley.com/terms-and-conditions) on Wiley Online Library for rules of use; OA articles are governed by the applicable Creative Commons License

lysimeter with a depth of 150 cm and a surface area of 1 m^2 filled with an undisturbed soil monolith (0–135 cm). At the bottom of the lysimeter, a 15 cm layer of purified quartz, sand, and gravel allowed free drainage to occur. The soil in the lysimeter was a loamy sandy Cambisol above moraine. Table 1 shows the basic physical and chemical parameters of the soil measured during the construction of the station in 2009. Reference methods for the measurement of the soil properties are described in Agroscope (2024). Soil water content was monitored using frequency domain reflectometry sensors (FDR; ThetaProbe ML2x, Delta-T Devices) at four depths (10, 30, 60 and 90 cm), each with two replicates, and averaged to daily values. Differences in recordings from the two sensor replicates were attributed to soil heterogeneities within the lysimeter column. Soil water suction was monitored using equilibrium tensiometers at 10 cm depth (EQ15, Ecomatic), and pressure transducer tensiometers (Tensio 150, UGT) at 30–90 cm depths. Weighting load cells (UGT WM 100, UGT, Münchenberg, Germany) with an accuracy of 0.01 mm of water on steel trusses were used to record the weights of the lysimeters at a temporal resolution of 5 min. The volume of seepage water was measured with tipping buckets installed at the bottom of the lysimeters. The actual evapotranspiration (AET) was derived from the water balance equation, as is typically done for lysimeters. There was no irrigation in the evaluated period, and the surface runoff was considered negligible. Consequently, AET was the result of precipitation, minus seepage water, minus the change in weight for the time period (Oberholzer et al. 2017).

In 2015 and 2021, silage maize was grown in the lysimeter, with a management of full fertilisation from mineral sources, at 100% of the recommended rate. From this lysimeter, validation data on AET, seepage water and soil water content were available and analysed in daily time steps. For calibrating the agro-hydrological models with the data of aboveground biomass of silage maize, we extended the dataset to include two other lysimeters, which had the same soil type and crop management. For an independent validation of yield simulations, a dataset from the above-cited variety trials was used (Figure 2).

2.2 | Model Descriptions

Four agro-hydrological models were chosen that mathematically represent two different numerical approaches for simulating the soil-crop-water dynamics. APEX version 1501 Rev.2203 (Gassman et al. 2009) and CANDY version 22.8.2 (Franko et al. 2024, 1995) (https://www.somod.info/candy_main.php) use a soil reservoir cascade scheme, whereas DAISY version 6.33 (Hansen et al. 1991) and SWAP version 4.2.0 (Kroes et al. 2000, 2017) use a numerical solution of the Richards equation.

The reservoir cascade approach applies to freely draining soils, in which groundwater has no influence on the soil water content in the rooting zone. There can be different levels of complexity in reservoir cascade models, but the most general

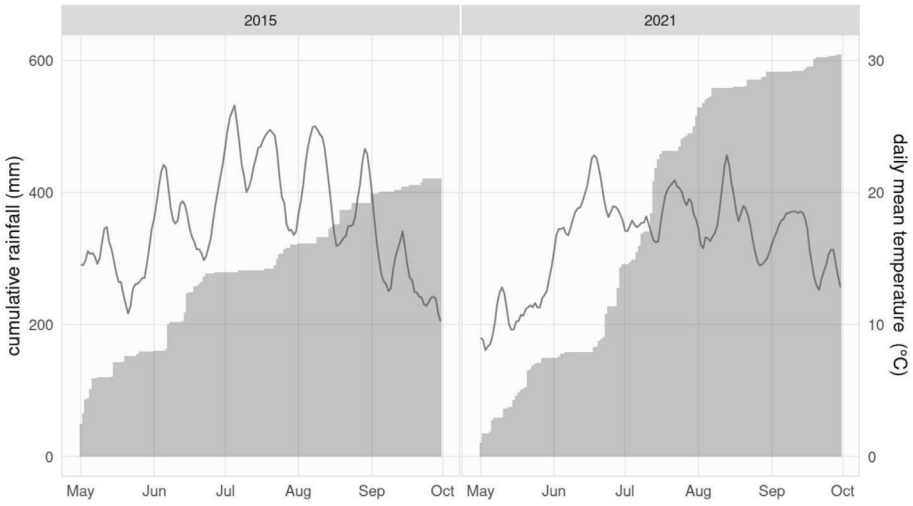

FIGURE 1 | Cumulative daily values of precipitation (mm) and mean daily temperature (°C) during the period of growth of silage maize in 2015 and 2021. Mean daily temperatures calculated with a moving average every 5 days.

TABLE 1 | Soil physical and chemical properties. PD: Particle density (g cm^{-3}), BD: Dry bulk density (g cm^{-3}), OC: Soil organic carbon (g 100 g^{-1}), $CACO_3$: Calcium carbonate (%), CEC: Cation exchange capacity (cmol$^+$ kg^{-1}).

Horizon	Depth cm	Clay %	Silt %	Sand %	PD g cm^{-1}	BD g cm^{-3}	OC g 100 g^{-1}	pH	$CaCO^3$%	CEC cmol$^+$ kg^{-1}
Ahp	0–25	16	32	51	2.63	1.46	0.99	6.9	0.1	9.81
Bcn	25–65	20	26	53	2.66	1.58	0.21	6.6	0.0	9.33
B (g) (t)	65–110	18	24	58	2.68	1.55	0.09	6.7	0.0	8.65
Bg (t)	110–135	16	27	57	2.69	1.62	0.05	6.8	0.0	7.45

13652389, 2025, 2, Downloaded from https://bsssjournals.onlinelibrary.wiley.com/doi/10.1111/ejss.70088 by Schweizerische Akademie Der, Wiley Online Library on [27/03/2025]. See the Terms and Conditions (https://onlinelibrary.wiley.com/terms-and-conditions) on Wiley Online Library for rules of use; OA articles are governed by the applicable Creative Commons License

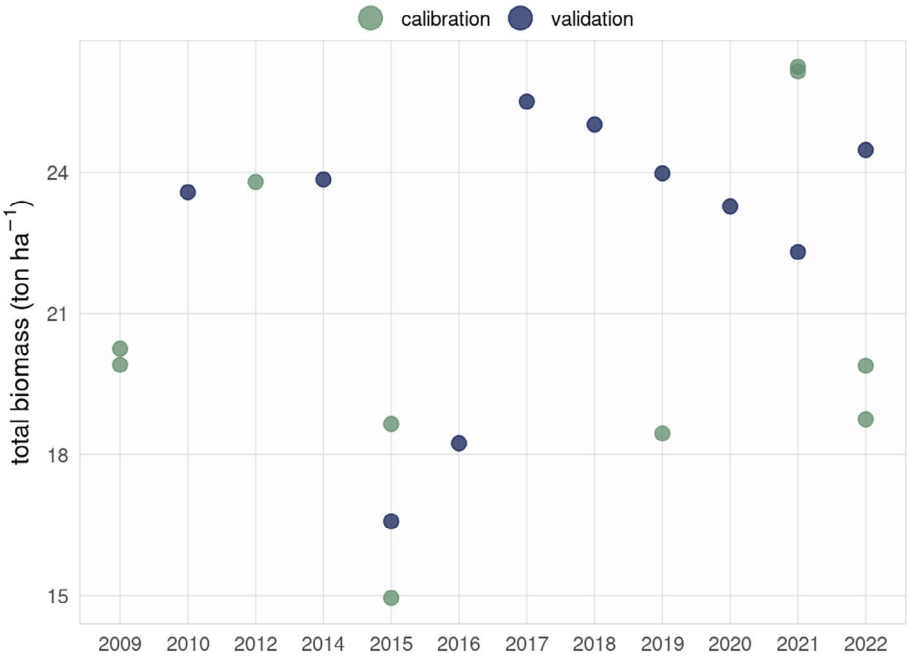

FIGURE 2 | Measured values of aboveground biomass between the years of 2009 and 2022 used for calibration and validation of the models. Calibration was performed with data from the lysimeters, and validation with data from variety trials.

concept is that the available water in the soil is stored between a lower (permanent wilting point, PWP) and an upper limit (field capacity, FC). The soil profile is composed of layers with distinct attributes that allow for water to flow from one layer to another.

The Richards-based description consists of the solution of a non-linear partial differential equation, most commonly in the vertical direction, with a sink term to represent the root water uptake:

$$C(h)\frac{\partial h}{\partial t} = \frac{\partial}{\partial z}\left[K(h)\frac{\partial (h+z)}{\partial z}\right] - S_a(h) \quad (1)$$

where $C(h)$ (cm^{-1}) is the specific water capacity, the derivative of the soil water retention function $\theta(h)$, which describes the relation between water content θ (cm^3 cm^{-3}) and soil water suction h (cm, defined as positive when $h > 0$), t (d) is time, $K(h)$ (cm d^{-1}) is the hydraulic conductivity as a function of h, z (cm) is the vertical spatial coordinate (negative downwards), and $S_a(h)$ (d^{-1}) is a sink term representing the rate of soil water extraction by plant roots.

In this approach, a mathematical relationship between $\theta(h)$ and $K(h)$ is essential to solve Equation (1). We used the Genuchten (1980)–Mualem (1976) equation to describe this relationship:

$$\Theta(h) = \frac{\theta - \theta_r}{\theta_s - \theta_r} = \frac{1}{\left[1 + |\alpha h|^n\right]^{1/n}}$$
$$K(h) = K_s \Theta^l \left[1 - \left(1 - \Theta^{n/(n-1)}\right)^{(n-1/n)}\right]^2 \quad (2)$$

where the relative degree of saturation is Θ is defined by the saturated (θ_s) and residual (θ_r) soil water contents (cm^3 cm^{-3}), α (cm^{-1}), n, and l are empirical shape parameters, and K_s is the saturated hydraulic conductivity (cm d^{-1}).

2.2.1 | General Setup of the Models

A homogenised soil parametrization and general workflow were used by all models to ensure a similar description of the crop development. For calibration of aboveground biomass, all four agro-hydrological models were run using soil parameters derived with the PTF developed by Weynants et al. (2009). This PTF was chosen because it is the PTF that solely considers soil texture, soil organic carbon and bulk density, which are all commonly identified as strong factors in the prediction of SHP (Looy et al. 2017). The maximum root depth was set to 135 cm, that is, the actual total depth of the soil in the lysimeter. Figure A2 shows the discretisation of the soil profile in each model as compared to the location of the sensors in the lysimeter. More details about sub-discretisation of layers are provided with the model descriptions below.

All models used local meteorological data as input, with a spin-up period starting on January 1st, 1981. The crop rotation in the four agro-hydrological models was defined as a silage maize monoculture without any crops grown during winter. Nitrogen stress was not considered, that is, we assumed optimal nitrogen supply throughout the growing season. The sowing dates were the same as the ones in the lysimeters for the years in which aboveground biomass data was available (2009, 2012, 2015, 2019, 2021, 2022), and according to the variety trials in the other years.

After adjusting the simulated crop phenology to match it with observed dates of flowering and maturity, additional crop parameters were calibrated to match simulated aboveground

13652389, 2025, 2, Downloaded from https://bsssjournals.onlinelibrary.wiley.com/doi/10.1111/ejss.70088 by Schweizerische Akademie Der, Wiley Online Library on [27/03/2025]. See the Terms and Conditions (https://onlinelibrary.wiley.com/terms-and-conditions) on Wiley Online Library for rules of use; OA articles are governed by the applicable Creative Commons License

biomass with observations from the lysimeters. The flowering dates simulated by DAISY and SWAP were defined as the date when the development stage (DVS) equals 1.0. For CANDY, the dates when the BBCH reaches 65 were chosen as this is usually when the flowering of maize occurs (range 61–69; Meier et al. (2001)). The simulated dates were compared with the flowering data available from variety trials (Figure A3).

2.2.2 | APEX

APEX (Agricultural Policy/Environmental eXtender) is a continuous, physically based, spatially explicit agro-hydrological model that runs on a daily time step (Izaurralde et al. 2006). Soil water flux is simulated on the basis of the reservoir cascade concept. The unsaturated hydraulic conductivity is calculated using a variable saturation hydraulic conductivity *VSHC* (4 mm slug) method, whereby the flow of water from one soil layer to the next layer occurs when FC (defined in APEX as the soil water content at a tension of 330 cm) in a soil layer is exceeded. The volume of mobile water in each soil layer of 4 mm is discretized into small fractional volumes of water, called slugs. Only if the available water is $>0.01\,cm^3\,cm^{-3}$ does the slug method take place. Percolation is iteratively simulated for each slug to discharge into the next 4 mm layer, until all slugs have moved into the sublayer (Doro et al. 2017). During each iteration, the effective hydraulic conductivity is calculated for each slug based on the saturated hydraulic conductivity, FC, porosity, soil characteristics and the actual soil water content, using a method similar to Gardner (1958). In addition to downward flux, an upward flux can occur, caused by evaporation or plant water uptake.

Potential evapotranspiration (PET) is calculated using the Penman–Monteith equation (Allen et al. 1998). Evaporation and transpiration are partitioned as described by Ritchie (1972). Actual soil water evaporation is simulated by using an exponential function related to soil depth and water content. The transpiration plus any evaporation due to canopy interception is simulated as a linear function of the potential evaporation and the leaf area index. The daily root growth is simulated as a function of the heat units (HU) and the crop potential maximum rooting depth (RDMX). The root depth (RD) per day (i) is a function of the soil profile depth (RZ) and is calculated as:

$$\mathrm{RD}(i) = min(2.5 \times \mathrm{RDMX}(i) \times \mathrm{HU}(i), \mathrm{RDMX}, \mathrm{RZ}). \quad (3)$$

Mineral fertiliser was applied according to the needs of the simulated silage maize, which was determined according to the biomass. To simulate the lysimeter, the soil layers in APEX were set up as per the soil horizons in the lysimeter to a depth of 135 cm, after which a 15 cm layer of coarse sand was added to simulate a total depth of 150 cm; this coarse sand layer allowed free draining of water to drain to the bottom of the lysimeter (seepage water).

A sensitivity analysis was performed to select potential parameters for calibration. A set of 31 parameters related to crop development were initially chosen based on a literature review (Baffaut et al. 2017; Jones et al. 2021; Mason et al. 2020; Wang et al. 2011). To calibrate the most influential parameters, a screening was undertaken using the Sobol' variance-based sensitivity analysis (Puy et al. 2022). A sample hyperspace was compiled with the 31 parameter values chosen by quasi-random numbers and a sample size of 5000 parameter sets. Quasi-random numbers were generated to compute the first order (Si) and total-order (Ti) Sobol' indices. Additionally, Sobol' indices for a dummy parameter were computed to estimate the numerical approximation error and identify non-influential parameters. Parameters with confidence intervals equal to or above the Si and Ti indices of the dummy parameter were sensitive. Based on the outputs, 12 sensitive parameters were selected for further calibration (Table 2). Next, using quasi-random number sampling, parameter sets were generated and 5000 runs were simulated. The dotty (point) plots were visually examined to set ranges for the final calibration. The calibration was carried out using the root mean square error (RMSE) of the corn silage yields for the years available as the objective function. The runs with the lowest RSME and a KGE >=0.3 were selected. APEX does not simulate an output of crop phenology (or growth stages). Instead, it provides daily increments of the above and below ground biomass. The plant development, including leaf area growth and senescence, and partitioning of dry matter into roots and shoots are simulated based on the daily heat units accumulated, whereby a total heat unit sum determines when the maize crop reaches maturity. The biomass accumulation is constrained by a crop growth factor; stresses caused by water, nutrients, temperature, aeration, and radiation. Plant water stress is calculated as the ratio of actual vs. potential daily plant water use. The water stress factor (PARM38, Table 2) limits biomass production, which is decreased in proportion to the reduction in transpiration (Hanks 1983).

2.2.3 | CANDY

CANDY is a deterministic, descriptive model that allows soil profiles down to 200 cm that are divided into 10 cm thick layers. Water flux is calculated using a reservoir cascade concept, that is, downwards flow of water into a lower soil layer is only simulated if the water storage exceeds FC (here defined as soil water content at $h = 63$ cm) of the layer above. This implies that the amount of water that could enter the soil system is given by the daily rainfall, but includes also irrigation and water added with manure or slurry applications. The water balance in CANDY is calculated assessing the availability in relation to the maximum (FC) and minimum water content (PWP). Consequently, the velocity of the downward flux of water is controlled by the saturated hydraulic conductivity through the drainage parameter λ_p (Koitzsch and Günther 1990).

$$\frac{\delta\theta}{\delta t} = -\lambda_p\left(\theta - \theta_{FC}\right)^2, \theta > \theta_{FC} \quad (4)$$

where θ is the soil water content ($cm^3\,cm^{-3}$) of a soil column of defined thickness, t is the time, and θ_{FC} is the water content at field capacity ($cm^3\,cm^{-3}$). Evaporation is considered to affect the upper five layers, that is, the top 50 cm of the soil profile, while all rooted layers are considered for calculating the transpiration. The calculation of both potential evaporation (PE), PET and AET ($mm\,d^{-1}$) is based on the work of Koitzsch and Günther (1990) and further presented on Franko et al. (1995):

13652389, 2025, 2, Downloaded from https://bsssjournals.onlinelibrary.wiley.com/doi/10.1111/ejss.70088 by Schweizerische Akademie Der, Wiley Online Library on [27/03/2025]. See the Terms and Conditions (https://onlinelibrary.wiley.com/terms-and-conditions) on Wiley Online Library for rules of use; OA articles are governed by the applicable Creative Commons License

TABLE 2 | APEX model parameters calibrated to simulate silage maize aboveground biomass. PARM3 sets the fraction of growing season when water stress starts by reducing HI. If PARM38 equals zero, the water stress is strictly a function of soil water content, if it is equals 1, water stress is strictly a function of AET/PET. Minimum and maximum thresholds represent the ranges used for the initial calibration.

Name	Description	Default	Min	Max	Units	Optimised value
HI	Harvest index	0.5	0.5	1.25	—	0.98
PARM3	Water stress-harvest index (HI).	0.75	0	1	—	0.55
PARM30	Heat effect on HI	1	1	10	—	8.24
PARM38	Water stress weight coefficient	1	0	1	—	0.47
PARM82	Related to percolation and lateral flow of 4 mm slug	3	1	6	—	2.43
WA	Biomass-Energy Ratio	39	19.5	58.5	$(kg\,ha^{-1})/(MJ\,m^{-2})$	54.53
DMLA	Maximum potential LAI	6	3.5	6	$m^2\,m^{-2}$	5.71
DLAI	Fraction of growing season when leaf area declines	0.8	0.72	0.88	—	0.74
TOP	Optimal temperature for growth	25	20	27.5	°C	20.08
TBS	Minimum temperature for growth	10	5	12.5	°C	10.64
RLAD	LAI decline rate parameter	1	0	10	—	6.46
RBMD	Biomass-energy ratio decline rate	1	0	10	—	8.97

$$\mathrm{PE} = 0.0041\left(T_{\mathrm{air}} + 22.7\right)(GR + 2.09) \tag{5}$$

$$\mathrm{PET} = \min\left(1 + 0.004ch, 1.4\right)PE \tag{6}$$

$$\mathrm{AET} = 0.5\min\left(\mathrm{PEI}, R_i\right) + \Psi H_1 \max\left(0, \left(1 - R_i/\mathrm{PEI}\right)\mathrm{PET}\right) + (1-\Psi)H_2\mathrm{PE} \tag{7}$$

where T_{air} is the air temperature (°C), GR is the daily sum of radiation energy ($MJ\,m^{-2}$), PEI is the potential evaporation of intercepted water by the crop ($mm\,d^{-1}$), ch is the crop height (cm), R_i is the intercepted water ($mm\,d^{-1}$), Ψ is the fraction of the soil surface that is covered by transpiring plants, and H_1 and H_2 are reduction coefficients, calculated as functions of the water content (Koitzsch and Günther 1990). Relevant processes of water flux are described for the unsaturated zone and without considering lateral fluxes. Surface runoff occurs as a result of infiltration surplus.

Crop growth is based on photosynthesis quantified by photosynthetic photon flux density $PPFD$ ($\mu mol\,m^{-2}\,s^{-1}$), based on the global radiation (GR, Wm^{-1}):

$$\mathrm{PPFD} = 2.3 \times 10^6 \frac{\mathrm{GR}}{86400} \tag{8}$$

The intercepted radiation PARX depends on leaf area index (LAI), canopy reflectance (refl) and the crop-specific k_{ex}, which is a development-dependent irradiance extinction coefficient. PARX is calculated as

$$\mathrm{PARX} = (1 - \mathrm{refl})\mathrm{PPFD}\frac{1 - exp\left(-k_{ex}LAI\right)}{k_{ex}LAI} \tag{9}$$

The daily photosynthesis rate (DPR) depends on PARX, the photosynthetic capacity (α), the photosynthetic rate at light saturation (β) and is further moderated depending on temperature stress (rf_T), water stress (rf_W), atmospheric CO_2 concentration (rf_C) and the nitrogen state of the crop (N_{leaf}) Huang et al. (2009):

$$\mathrm{DPR} = \frac{\alpha rf_T rf_W N_{leaf}\mathrm{PARX}}{\beta\mathrm{PARX}} \tag{10}$$

Water stress (rf_W) is calculated as follows:

$$rf_W = \min\left(1, \max\left(0.1, \frac{\sum_i \theta_i - \sum_i \mathrm{PWP}_i}{\sum_i FC_i - \sum_i \mathrm{PWP}_i}\right)\right) \tag{11}$$

where i is the evaluated day and PWP_i refers to the water content at which uptake of N by the plant ceases.

Root growth is controlled by the assimilate distribution, which in turn is described by a development index (DVI)-dependent partitioning factor. The amount of biomass that is distributed to the roots is transformed into root depth via a user-specific parameter (prx) until a maximum rooting depth is reached. In CANDY, the rooting depth of 135 cm cannot be assigned, since the compartments vary only each 10 cm, so the maximum rooting depth was set at 130 cm.

For this study, the *lysimeter setup* was used, implying that surface runoff was disabled and therefore all rainfall water eventually infiltrates the soil profile. The depth of the soil profile was set at 135 cm, and an additional 15 cm of coarse sand was assumed at the bottom boundary, as described by Prasuhn et al. (2016). CANDY allows the usage of different plant modules, some of which are N-uptake driven and require the

13652389, 2025, 2, Downloaded from https://bsssjournals.onlinelibrary.wiley.com/doi/10.1111/ejss.70088 by Schweizerische Akademie Der, Wiley Online Library on [27/03/2025]. See the Terms and Conditions (https://onlinelibrary.wiley.com/terms-and-conditions) on Wiley Online Library for rules of use; OA articles are governed by the applicable Creative Commons License

expected (or observed) crop yield as input data. However, for this study, a generic plant development model (*AGRO1*) inspired by the AGRO-C model (Huang et al. 2009) was used. Crop development was quantified by the development index DVI calculated from the daily mean temperature and an accumulated reference temperature (*ref_ts*). For phenology, parameters describing the temperature sums until emergence (*ts_emg*) and maturity (*ref_ts*) were set to 110 and 1100, respectively. In addition, the senescence parameter (senescence) was increased from 0.004 to 0.012. Parameter adaptation was done manually by comparing the simulated results with the observed aboveground biomass and the date of flowering (see Table 3).

2.2.4 | DAISY

DAISY is an agro-hydrological model (Abrahamsen and Hansen 2000) that simulates the fluxes of water, nitrogen, carbon and pesticides in agricultural fields (Hansen et al. 1991). The model simulates processes in the vadose zone, ranging from the top of the canopy to the bottom of the root zone, including water flow in the soil, solute flow, soil organic matter turnover and soil-vegetationvegetation-atmosphere transfer. For this study, DAISY version 6.33 (Hansen et al. 1991) was set up to use the Mualem–van Genuchten (Equation 2) parameters to simulate the hydrological processes described with the Richards equation (Equation 1). The bottom boundary was set up as a lysimeter, which means that there is free drainage to an open seepage face. The soil profile was set as the layers in Table 1, with sub-compartments of 1 cm. The crop was set up not to be affected by nitrogen stress, but water stress could occur. Water stress is a reducing factor in DAISY, where the value can range between 0 (no water stress) and 1 (no production). This function is activated when the root system cannot fulfil the demand for water from the canopy. The PET is calculated through the Penman-Monteith (Allen et al. 1998) method, based on the meteorological conditions. The AET was calculated by the default internal protocol in DAISY (Hansen 1984). Root growth in DAISY is mainly simulated by two penetration parameters: a rate, PenPar1 [cm dg^{-1} C d^{-1}, default 0.25] and a constant: PenPar 2 [dg C, default 4]. The growth rate of the root, PenPar1, can be limited by the soil water content of the soil, the clay content, and the developmental stage of the plant. The limiting factor can range from 0 to 1, following a linear function, and it was kept on its default parameters. The selection of parameters was based on the sensitivity analysis performed by (Wallach et al. 2021). For the phenology, the parameters *EmrTSum* were changed from 300 to 110 and *DSRate1* from 0.024 to 0.023 to ensure that the modelled phenology matched the measured phenology. For the calibration of the aboveground biomass in DAISY, the DEoptim package (v 2.2–8) (Mullen et al. 2011) in R (R Core Team 2024) was used (Table 4).

2.2.5 | SWAP

SWAP (soil water atmosphere plant) (Kroes et al. 2000, 2017) is a 1-D vertically directed agro-hydrological model that simulates the transport of water, solutes, and heat in the zone between the groundwater and the top of the plant canopy in variably saturated soils. Leaf photosynthesis and crop growth are calculated using the generic crop growth module WOFOST (WOrld FOod STudies) (Wit et al. 2019). The water content in a layered soil is calculated by applying the Richards

TABLE 3 | Parameters used in the calibration of CANDY.

Name	Description	Default	Min	Max	Unit	Adapted value
α	photosynthetic capacity per unit leaf nitrogen	27	—	—	μmol CO^2 s^{-1} $(gN)^{-1}$	22
β	photosynthetic rate at light saturation	60	—	—	μmol CO^2 m^{-2} s^{-1}	90
ts_emg	temperature sum until emergence	200	—	—	°C	110
ref_ts	temperature sum until maturity	700	—	—	°C	1100
senescence	partial LAI breakdown	0.004	—	—	—	0.012
sp_lf_ar	specific leaf area	0.008	—	—	$m^2 kg^{-1}$	0.01

TABLE 4 | Parameters used in the calibration of DAISY (Hansen et al. 1991), the range was used in the aboveground biomass calibration with DEoptim (Mullen et al. 2011).

Name	Description	Default	Min	Max	Unit	Adapted value
Fm	Maximum assimilation rate	6	2	10	g CO^2 m^{-2} h^{-1}	5.45
Qeff	Quantum efficiency at low light	0.04	0.001	0.1	g CO^2 m^{-2} h^{-1}/(W m^{-2})	0.09
E_Leaf	Conversion efficiency, leaf	0.68	0.1	1	g DM C/g Assimilated C	0.69
E_Stem	Conversion efficiency, stem	0.66	0.1	1	g DM-C/g Assimilated C	0.74
LeafAIMod	Specific leaf area modifier at DVS = 2 (maturity)	1	0.5	3	—	0.65

Note: DVS = 2 is the development stage at maturity.

13652389, 2025, 2, Downloaded from https://bsspjournals.onlinelibrary.wiley.com/doi/10.1111/ejss.70088 by Schweizerische Akademie Der, Wiley Online Library on [27/03/2025]. See the Terms and Conditions (https://onlinelibrary.wiley.com/terms-and-conditions) on Wiley Online Library for rules of use; OA articles are governed by the applicable Creative Commons License

equation with a sink term representing root water extraction (Equation 1).

For modelling silage maize in the lysimeter, AET and its separation between evaporation and transpiration were calculated using basic weather data using the Penman–Monteith method (Allen et al. 1998). Pounding was not allowed, meaning that all water precipitated would be directly converted to either infiltration or runoff. The bottom boundary condition was set as free outflow at soil-air interface, as recommended for lysimeters. Hysteresis, preferential flow, drainage, solute transport, snow and frost were not considered. The model did not considered neither nutrient stress nor salinity stress. The soil profile was described according to the natural layers in Table 1, with sub compartments varying from 0.5 cm in the topsoil to 5.0 cm in the bottom of the profile. Seepage water was considered as the water flux at the bottom of the soil profile (135 cm). The timing of harvest was set to depend on end of growing period, matching harvesting dates from the lysimeter management data. The plant water stress to oxygen was calculated according to Bartholomeus et al. (2008) and drought stress according to Feddes et al. (1978), with default values from the detailed crop file for maize in SWAP. Root development was set as a function of the initial rooting depth (10 cm), the maximum daily increase (2.2 cm d^{-1}), and the maximum rooting depth, and its increase was related to relative dry matter accumulation and affected by drought stress.

For the crop file calibration, the temperature sums (base 10°C) were calibrated with data from the silage maize variety trial (Section 2.1) and were shown to have an average value of 750°C-d from emergence to anthesis and 972°C-d from anthesis to maturity. The temperature needed for crop emergence was 110°C-d, with a temperature base of 4°C.

Initial crop parameters were obtained from the WOFOST crop file database (GitHub: Parameter sets for the WOFOST crop simulation model implemented in YAML) for the "temperate maize" variety. Those were optimised against the lysimeter yield data using differential evolution with the R package DEoptim (R Core Team 2024; Mullen et al. 2011). From the selected parameters, the optimised values of EFF, SPAN, CVO and CVS presented values at their minimum or maximum boundaries, indicating that an optimal solution would be found only beyond the biologically meaningful ranges defined for the calibration (Table 5).

2.3 | Pedotransfer Functions

An ensemble of 18 continuous PTFs was used in the model validation and comparison. Continuous PTFs were chosen because they provide the parameters of the SHP, instead of punctual values of water content or hydraulic conductivity, which were important for maintaining the consistency between agro-hydrological models. We tested different PTFs suggested by Nasta et al. (2021), including Szabó et al. (2021) and the PTFs presented by Weynants et al. (2009) and Wösten et al. (1999), which were cited as the most accurate in European soils. In addition, we tested the widely used Rosetta's functions Schaap et al. (2001, 2004) and Zhang and Schaap (2017). Table 6 shows an overview of all PTFs tested and the required input variables for each.

2.4 | Model Calibrations, Validations and Evaluations

We calibrated all four agro-hydrological models using yearly aboveground biomass (kg ha^{-1}) observed at 3 lysimeters and validated the models using aboveground biomass observed at the variety trials with silage maize (Figure 2). For the calibration, the modelling groups had access to the measured yearly above ground biomass from the lysimeters and phenology data from the variety trials, but not to the validation data of aboveground biomass, nor the evaluation data on AET, seepage water or soil water content from the lysimeter. The fit between measured and simulated values was assessed with the performance metric *d* (Willmott 1981), which varies from 0 to 1, with 1 being a perfect fit between the simulated data and the measured data.

TABLE 5 | Parameters used in the calibration of SWAP (Kroes et al. 2017), the ranges represent the maximum and minimum limits used in DEoptim.

Name	Description	Default	Min	Max	Unit	Adapted value
RSC	Minimum canopy resistance	130.0	30.0	300.0	s m^{-1}	30.2
SPAN	Life span under leaves under optimum conditions	33.0	24.8	41.3	d	24.8
SLATB	Specific leaf area at DVS = 0.0	0.0026	0.0016	0.0029	ha kg^{-1}	0.00286
AMAXTB	Max CO_2 assimilation rate at DVS = 2.0	5.0	0.0	40.0	kg ha^{-1} h^{-1}	1.825
KDIF	Extinction coefficient for diffuse visible light	0.600	0.480	0.720	—	0.583
EFF	Light use efficiency for real leaf	0.450	0.360	0.540	kg ha^{-1} h^{-1} $(Jm^2s)^{-1}$	0.540
CVO	Efficiency of conversion into storage organs	0.671	0.537	0.805	kg kg^{-1}	0.805
CVS	Efficiency of conversion into stems	0.658	0.526	0.790	kg kg^{-1}	0.789

13652389, 2025, 2, Downloaded from https://bsssjournals.onlinelibrary.wiley.com/doi/10.1111/ejss.70088 by Schweizerische Akademie Der, Wiley Online Library on [27/03/2025]. See the Terms and Conditions (https://onlinelibrary.wiley.com/terms-and-conditions) on Wiley Online Library for rules of use; OA articles are governed by the applicable Creative Commons License

TABLE 6 | Summary of PTFs used to determine soil hydraulic parameters.

Method	Input data	Reference
EUPTF01	texture + depth	Szabó et al. (2021)
EUPTF02	texture + depth + OC	
EUPTF04	texture + depth + $CACO_3$	
EUPTF05	texture + depth + pH	
EUPTF06	texture + depth + CEC	
EUPTF12	texture + depth + BD + pH	
EUPTF13	texture + depth + BD + CEC	
EUPTF20	texture + depth + OC + $CACO_3$ + pH	
EUPTF21	texture + depth + OC + $CACO_3$ + CEC	
EUPTF23	texture + depth + BD + $CACO_3$ + pH	
EUPTF27	texture + depth + OC + BD + $CACO_3$ + pH	
EUPTF28	texture + depth + OC + BD + $CACO_3$ + CEC	
EUPTF29	texture + depth + OC + BD + pH + CEC	
Rosetta1	texture + BD	Schaap et al. (2001)
Rosetta2	texture + BD	Schaap et al. (2004)
Rosetta3	texture + BD	Zhang and Schaap (2017)
WEYN2009	texture + BD + OC	Weynants et al. (2009)
WOST1999	texture + BD + OC + depth	Wösten et al. (1999)

Note: Texture: clay, sand and silt content (%), depth: average depth of the soil profile (cm), OC: soil organic carbon (g $100\,g^{-1}$), $CACO_3$: calcium carbonate (%), CEC: cation exchange capacity ($cmol^+kg^{-1}$), BD: dry bulk density ($g\,cm^{-3}$).

To evaluate the possible under- or over-estimation of the models, we used the pbias (Zambrano-Bigiarini 2024), which varies from $-\infty$ (model underestimates the data) to $+\infty$ (model overestimates the data). A perfectly unbiased model presents a pbias equal to zero. The Nash–Sutcliffe efficiency (NSE) was calculated for the daily outputs and varies from $-\infty$ to 1, with 1 showing that the model perfectly fits the data. If the NSE is less than 0, the mean of the measured values represents a better performance than the model (Nash and Sutcliffe 1970). The performances of the calibrated models parametrized with the 18 PTFs were evaluated based on measured daily values of AET ($cm\,d^{-1}$), seepage water ($cm\,d^{-1}$) and soil water content ($cm^3\,cm^{-3}$) at 10, 30, 60 and 90 cm depths obtained from one lysimeter with maize for one dry year (2015) and one wet year (2021).

2.5 | ANOVA-Based Variance Partitioning

We used ANOVA (analysis of variance) to attribute the contribution of the factors model and PTF to the simulated outputs described in Section 2.4, as done for example Li et al. (2023). The used variables of interest (y) were the accumulated annual values of: aboveground biomass ($kg\,ha^{-1}y^{-1}$), transpiration ($mm\,y^{-1}$), evaporation ($mm\,y^{-1}$) and seepage water ($mm\,y^{-1}$). For the soil water content ($cm^3\,cm^{-3}$), y refers to simulated outputs at a daily resolution and at depths of 10, 30, 60 and 90 cm. ANOVA quantifies the impacts of each independent factor (model and PTF) and their interactive effects on the dependent output (y), and is given by the relationship:

$$y_{ij} = \mu + \alpha_{\mathrm{PTF}_k} + \beta_{\mathrm{model}_j} + \gamma_{\mathrm{interaction}_{kj}} \tag{12}$$

where y_{ij} is the value of the response variable (y) for the i-th observation under the k-th level of PTF and the j-th level of model, μ is the overall mean of y, α_{PTF_k} is the contribution of the factor PTF, β_{model_j} is the contribution of the factor model and $\gamma_{\mathrm{interaction}_{kj}}$ is the contribution of the interaction between PTF and model. Each component is calculated as:

$$\mu = \frac{1}{n}\sum_{i=1}^{n} y_i \tag{13}$$

$$\alpha_{\mathrm{PTF}_k} = \bar{y}_{\mathrm{PTF}_k} - \mu \tag{14}$$

$$\beta_{\mathrm{model}_j} = \bar{y}_{\mathrm{model}_j} - \mu \tag{15}$$

$$\gamma_{\mathrm{interaction}_{kj}} = \bar{y}_{\mathrm{PTF}_k,\mathrm{model}_j} - \left(\mu + \alpha_{\mathrm{PTF}_k} + \beta_{\mathrm{model}_j}\right) \tag{16}$$

where n is the total number of PTF and model combinations ($n = 4$ models × 18 PTFs), $\bar{y}_{\mathrm{PTF}_k}$ is the mean of y for the k-th level of PTF, $\bar{y}_{\mathrm{model}_j}$ is the mean of y for the j-th level of model, and $\bar{y}_{\mathrm{PTF}_k,\mathrm{model}_j}$ is the mean of y for the combination of k-th level of

13652389, 2025, 2, Downloaded from https://bsssjournals.onlinelibrary.wiley.com/doi/10.1111/ejss.70088 by Schweizerische Akademie Der, Wiley Online Library on [27/03/2025]. See the Terms and Conditions (https://onlinelibrary.wiley.com/terms-and-conditions) on Wiley Online Library for rules of use; OA articles are governed by the applicable Creative Commons License

PTF and j-th level of model. In the ANOVA, the total sum of squares (TSS) is used to quantify how much the obtained values deviate from μ, given by:

$$\mathrm{TSS} = \sum_{i=1}^{n} \left(\mathrm{y}_i - \mu\right)^2 \tag{17}$$

where y_i is the observed value of the response variable for the i-th observation. Given the two evaluated factors, TSS can be decomposed:

$$\mathrm{TSS} = \mathrm{SS}_{\mathrm{PTF}} + \mathrm{SS}_{\mathrm{model}} + \mathrm{SS}_{\mathrm{interaction}} + \mathrm{SS}_{\mathrm{Residuals}} \tag{18}$$

where $\mathrm{SS}_{\mathrm{PTF}}$ is the contribution of the factor PTF, $\mathrm{SS}_{\mathrm{model}}$ is the contribution of the model, $\mathrm{SS}_{\mathrm{interaction}}$ is the contribution due to the interaction between model and $\mathrm{SS}_{\mathrm{residuals}}$ is the unexplained variance or 'noise'. In our case, since there was only one output y per year (or per day), $\mathrm{SS}_{\mathrm{residuals}}$ was zero, since all the variance in the results can be explained by the PTF, model or their interaction. Each contribution of TSS is described as:

$$\mathrm{SS}_{\mathrm{PTF}} = \sum \left(\hat{y}_{\mathrm{PTF}} - \mu\right)^2 \tag{19}$$

$$\mathrm{SS}_{\mathrm{model}} = \sum \left(\hat{y}_{\mathrm{model}} - \mu\right)^2 \tag{20}$$

$$\mathrm{SS}_{\mathrm{interaction}} = \sum \left(\hat{y}_{\mathrm{interaction}} - \hat{y}_{\mathrm{PTF}} - \hat{y}_{\mathrm{model}} + \mu\right)^2 \tag{21}$$

where $\hat{y}_{\mathrm{PTF}}$ is the predicted value based on the main effect of PTF, $\hat{y}_{\mathrm{model}}$ is the predicted value based on the main effect of model, and $\hat{y}_{\mathrm{interaction}}$ is the predicted value based on the combination of PTF and model. See Appendix A5 for the decomposition of the contributions in ANOVA.

3 | Results

3.1 | Soil Hydraulic Parameters

The soil hydraulic parameters (SHP) predicted by the pedotransfer functions (PTF) at each evaluated depth presented similar curve slopes for both soil water retention and soil hydraulic conductivity (Figures 3 and 4). Soil water content estimations varied between 0.05–0.08 $\mathrm{cm^3\,cm^{-3}}$ in both the wet and dry ranges of the retention curves. Soil hydraulic conductivity curves also suggested that the choice of PTF affects the unsaturated hydraulic conductivity to a larger degree in drier soil conditions (Figure 4). At the drier end, a lower soil hydraulic conductivity was obtained by the three Rosetta PTF models (Schaap et al. 2001, 2004; Zhang and Schaap 2017), whereas close to saturation, the rates of

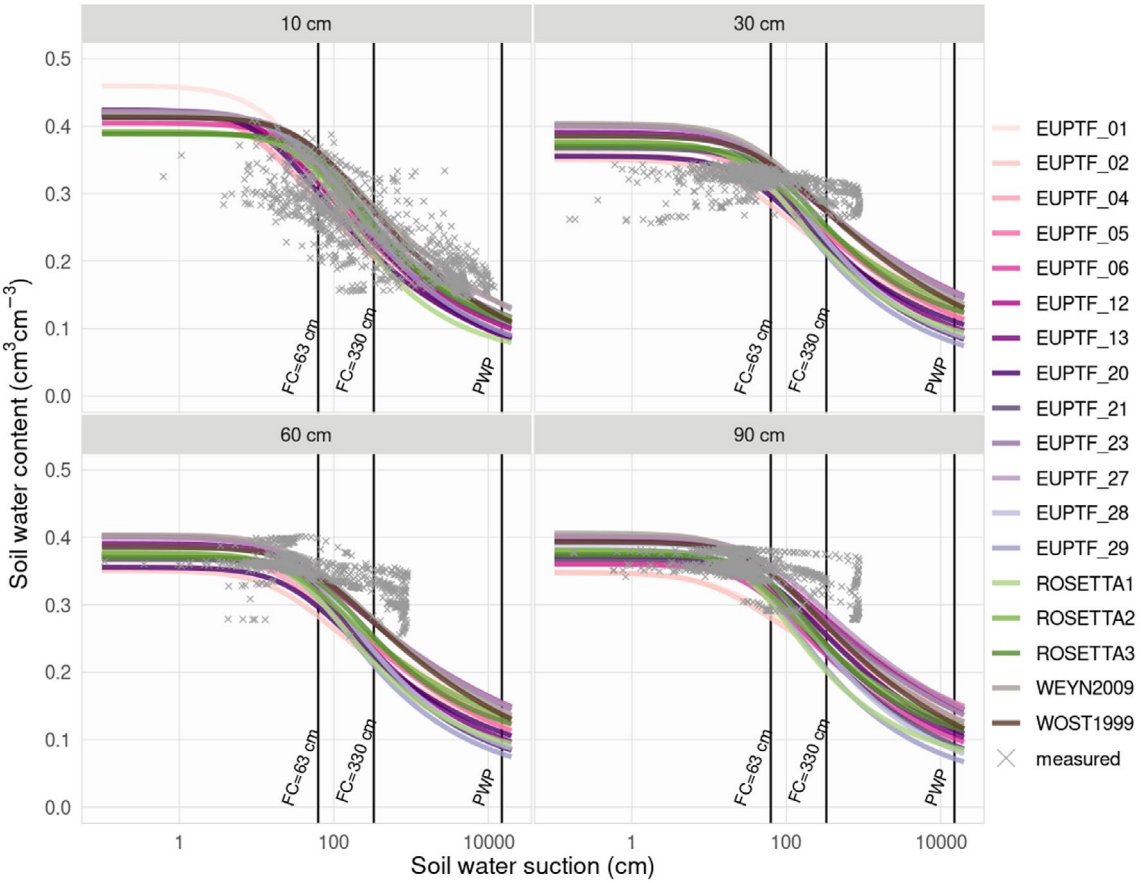

FIGURE 3 | Soil water retention curves estimated by PTFs at the soil depths of 10, 30, 60 and 90 cm. Crosses represent the measured soil water content versus soil water suction monitored at the lysimeters. Vertical lines highlight the soil water suction at field capacity (FC) and permanent wilting point (PWP).

13652389, 2025, 2, Downloaded from https://bsssjournals.onlinelibrary.wiley.com/doi/10.1111/ejss.70088 by Schweizerische Akademie Der, Wiley Online Library on [27/03/2025]. See the Terms and Conditions (https://onlinelibrary.wiley.com/terms-and-conditions) on Wiley Online Library for rules of use; OA articles are governed by the applicable Creative Commons License

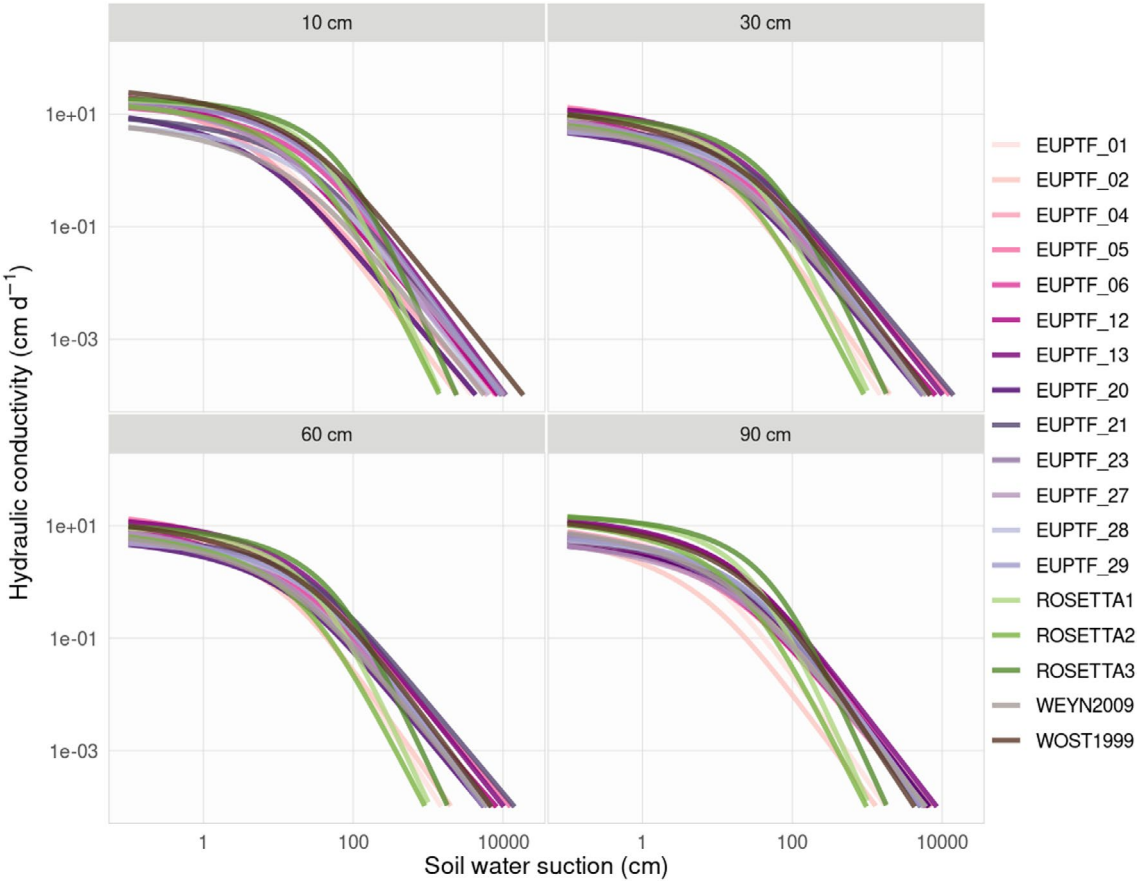

FIGURE 4 | Soil hydraulic conductivity curves estimated by PTFs at the soil depths of 10, 30, 60 and 90 cm.

hydraulic conductivity were similar amongst all PTFs. To check the plausibility of the PTF estimations, Figure 3 presents the measured soil water content versus soil water suction measured in the lysimeters during the years when silage maize was grown. The measured points are in the same range as the model simulations, despite a large cloud of uncertainty in the measured data.

3.2 | Calibration and Validation of Aboveground Biomass and Phenology

Table 7 provides a summary of the four agro-hydrological model performances in simulating aboveground biomass for silage maize in the calibration and validation steps. The results showed that most models were able to reproduce observed biomass levels and inter-annual variability of biomass production with reasonable accuracy for both the calibration and validation data. However, CANDY tended to underestimate the observed yields (pbias = −15.9) and showed a weaker performance compared to the other models. All models tended to simulate lower aboveground biomasses in the validation period. Regarding the simulation of phenological development, CANDY ($d = 0.65$), DAISY ($d = 0.73$) and SWAP ($d = 0.72$) showed good agreement with observed flowering dates (Figure A3). For APEX, no comparison with observed flowering dates could be made because flowering is not explicitly determined in the model.

TABLE 7 | Metrics for calibration and validation of aboveground biomass simulated by all models.

	Calibration		Validation	
Model	***d***	**pbias**	***d***	**pbias**
APEX	0.81	5.1	0.66	−6.3
CANDY	0.22	−15.9	0.20	−18.2
DAISY	0.87	−3.9	0.37	−10.1
SWAP	0.72	−2.1	0.56	−4.3

Note: Calibration considers only the soil parametrization with the PTF developed by Weynants et al. (2009) as compared with the lysimeter data; validation considers all PTFs compared with yield data from the variety trials.

3.3 | Model Evaluations

To explore the propagation of uncertainties due to the choice of PTF on the simulated model outputs in the four different agro-hydrological models, Figures 5–7 show the simulated soil water content in the top- and sub-soil layers, AET and seepage water, both for the dry year 2015 and the wet year 2021. In these graphs, the ranges of model estimates produced with different PTF parameterisations are indicated by shaded bands.

Figure 5 shows that all models were able to capture the observed dynamics reasonably well at all of the evaluated depths and years, although model performance tended to decrease in the two lower

13652389, 2025, 2, Downloaded from https://bsssjournals.onlinelibrary.wiley.com/doi/10.1111/ejss.70088 by Schweizerische Akademie Der, Wiley Online Library on [27/03/2025]. See the Terms and Conditions (https://onlinelibrary.wiley.com/terms-and-conditions) on Wiley Online Library for rules of use; OA articles are governed by the applicable Creative Commons License

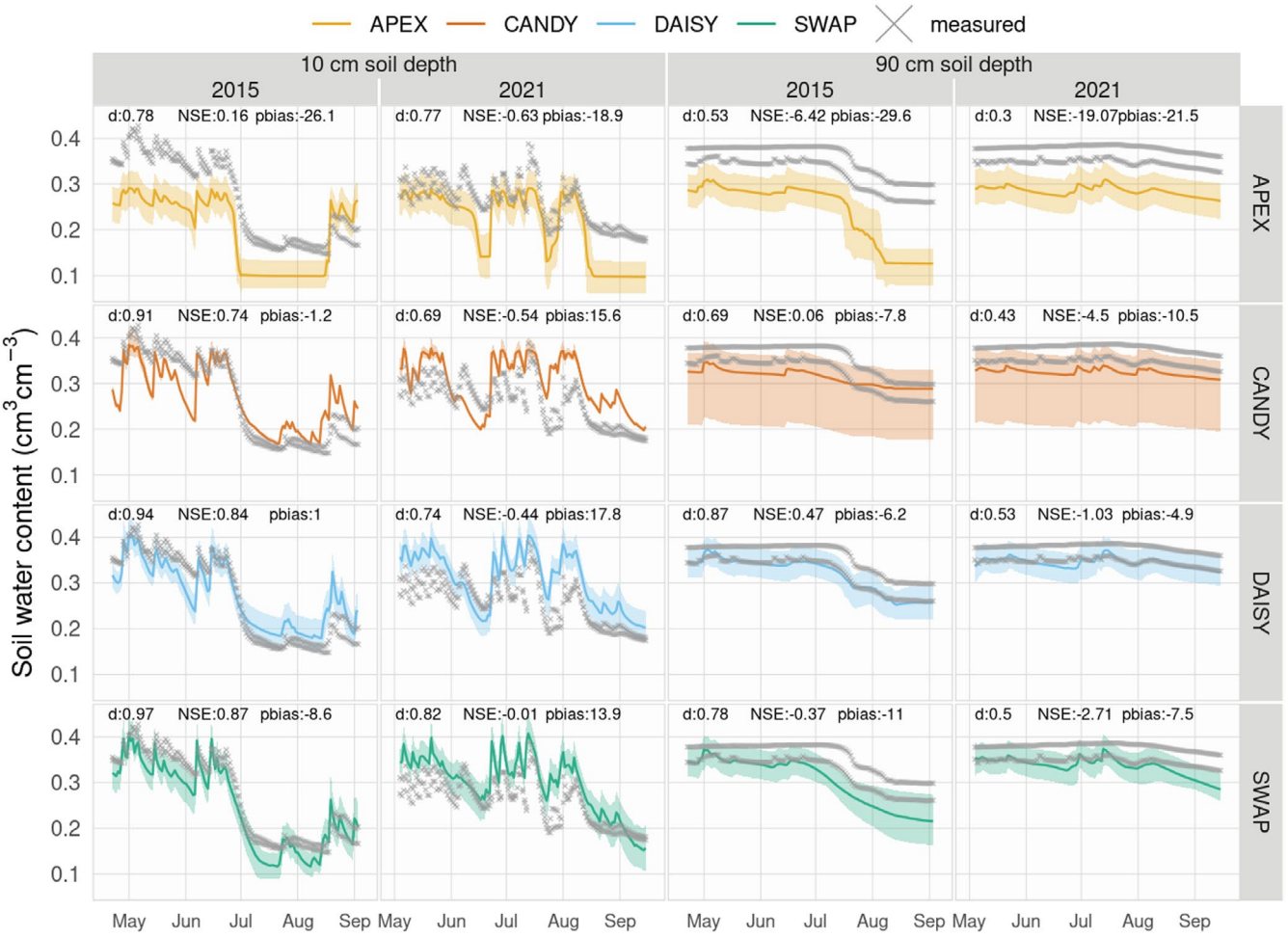

FIGURE 5 | Measured soil water content (grey crosses) over a dry (2015) and a wet (2021) year at two soil depths (panel columns) in comparison to soil water contents simulated with each of the four models (panel rows). Coloured full lines indicate mean values derived with all PTFs, shading indicates the full range between minimum and maximum. Metrics are calculated based on the average value from the PTF ensemble including two sensors per depth.

layers of 60 and 90 cm (Figures A6 and A7). The simulated soil water contents were sensitive to the choice of PTF in all models, as shown by their shaded areas in Figure 5. It was also interesting to note that the soil water content simulated by CANDY was largely unaffected by PTF choice at 10 cm depth, but the sensitivity increased over 30, 60 and 90 cm depth. In the bottom layers of the soil profile (90 cm), all models underestimated the measured soil water contents in the lysimeters, as indicated by the negative pbias's. APEX showed the strongest underestimations of water content in both years and all depths, as shown by consistently negative pbias (Figure 5). Despite a general tendency of all models to underestimate the soil water content, during the wet summer of 2021, the soil water content tended to be overestimated by three of the four models (CANDY, DAISY SWAP). However, all models were able to represent the soil water content dynamics well, both at the 10 and 90 cm depths. APEX simulated the greatest fluctuations in soil water content during the growing season and tended to have rapid soil drying once the water content dropped below about 0.2 $cm^3 cm^{-3}$.

Figure 6 shows the simulated AET, as well as the PET as calculated by each model. The difference between PET and AET indicates a stress caused most likely by dry soil conditions. All models performed well in representing both the levels and the dynamics of AET, with consistently positive NSEs (except CANDY in 2015). All models except CANDY perform better in the dry year (2015) than in the wet year (2021), where the high AET values measured during the late summer of 2021 were not matched by any of the four models. For estimating AET, the sensitivity of the models to the choice of PTF was overall low in comparison to the simulated soil water contents. Despite overall good simulations during the growing season, CANDY produced unusually high estimations of AET already at the beginning of the growing season, indicating limitations in the model approach for calculating AET. The two Richards-based models DAISY and SWAP showed the highest sensitivity of AET estimates to PTF choices—mostly during dry periods as in the summer of 2015. Considering the cumulative estimations of AET (Figure A4), CANDY and SWAP overestimate AET in the dry year 2015 (pbias > 20), but perform well in the wet year 2021. In contrast, APEX and DAISY underestimated daily AET in the wet year (negative pbias), but matched observed daily AET in the dry year with only small pbias (+/− 0.4%). Compared to daily AET estimates (Figure 6), seasonal sums of AET show a much stronger sensitivity to the choice of PTF (particularly

13652389, 2025, 2, Downloaded from https://bsssjournals.onlinelibrary.wiley.com/doi/10.1111/ejss.70088 by Schweizerische Akademie Der, Wiley Online Library on [27/03/2025]. See the Terms and Conditions (https://onlinelibrary.wiley.com/terms-and-conditions) on Wiley Online Library for rules of use; OA articles are governed by the applicable Creative Commons License

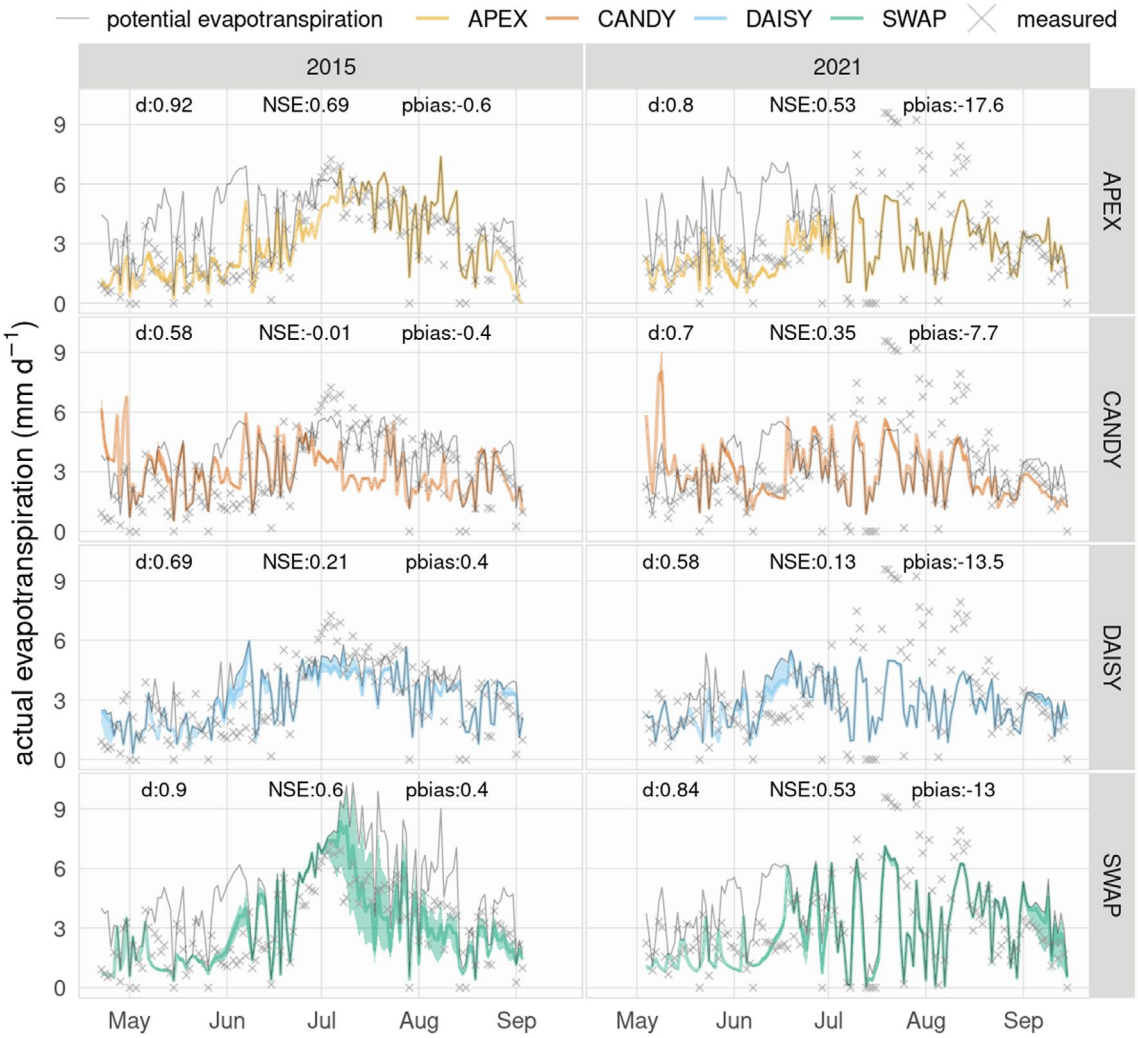

FIGURE 6 | Measured actual evapotranspiration (grey crosses) over a dry (2015) and a wet (2021) year (panel columns) in comparison to potential and actual evapotranspiration simulated with each of the four models. Coloured full lines indicate mean values derived from all PTFs, shading indicates the range between minimum and maximum. Metrics are calculated based on the average value from the PTF ensemble.

evident in SWAP estimates, see Figure A4). This is explained by the fact that daily differences in AET originating from the choice of PTF accumulate over the growing season.

Figure 7 shows that the dynamics of measured seepage water generation were matched by all models with reasonable accuracy in both evaluated years. SWAP simulated the highest peaks in daily seepage and showed a high sensitivity to PTF choice (as indicated by the shaded bands in Figure 7). For the other models, the influences of PTF choice on daily seepage were considerably smaller. Considering cumulative values of the simulated seepage water (Figure A5), SWAP and APEX showed sensitivity to the choice of PTF, although SWAP had higher sensitivity. APEX simulated the cumulative amount of seepage well in the wet year (Figure A5), despite a lower performance in simulating the seasonal dynamics (Figure 7). On the other hand, CANDY predicted the seasonal dynamics of seepage water well but underestimated the cumulative seepage water in both dry and wet conditions (Figure A5).

All model simulations of the soil water content showed a high sensitivity to the choice of PTF (Figure A11). However, except for SWAP, the propagation of the sensitivities to the other simulated outputs was barely observed; this was especially true for the crop-related outputs of aboveground biomass and AET. This discrepancy between model sensitivity can be explained by differences in simulated canopy development affecting crop water demand and root water uptake (see LAI and rooting depth graphics in appendix A12 and A13). We expected a higher sensitivity of the results from DAISY to the PTFs, but the fact that LAI and rooting depth development were strongly affected by PTF choice in SWAP, while it remains mostly unaffected in DAISY, can also explain why variance in AET estimates was generally higher in SWAP than in DAISY. For the two reservoir cascade models APEX and CANDY, the simulated evapotranspiration was largely insensitive to PTF choices.

Considering the full ensemble of four models and 18 PTFs, the performance metrics achieved were very good with regard to all simulation outputs, with NSE = 0.61 for AET (d = 0.84, pbias = −7%), NSE = 0.52 for seepage water (d = 0.79, pbias = −3%) and NSE = 0.55 for soil water content (d = 0.88, pbias = −8%).

13652389, 2025, 2, Downloaded from https://bsssjournals.onlinelibrary.wiley.com/doi/10.1111/ejss.70088 by Schweizerische Akademie Der, Wiley Online Library on [27/03/2025]. See the Terms and Conditions (https://onlinelibrary.wiley.com/terms-and-conditions) on Wiley Online Library for rules of use; OA articles are governed by the applicable Creative Commons License

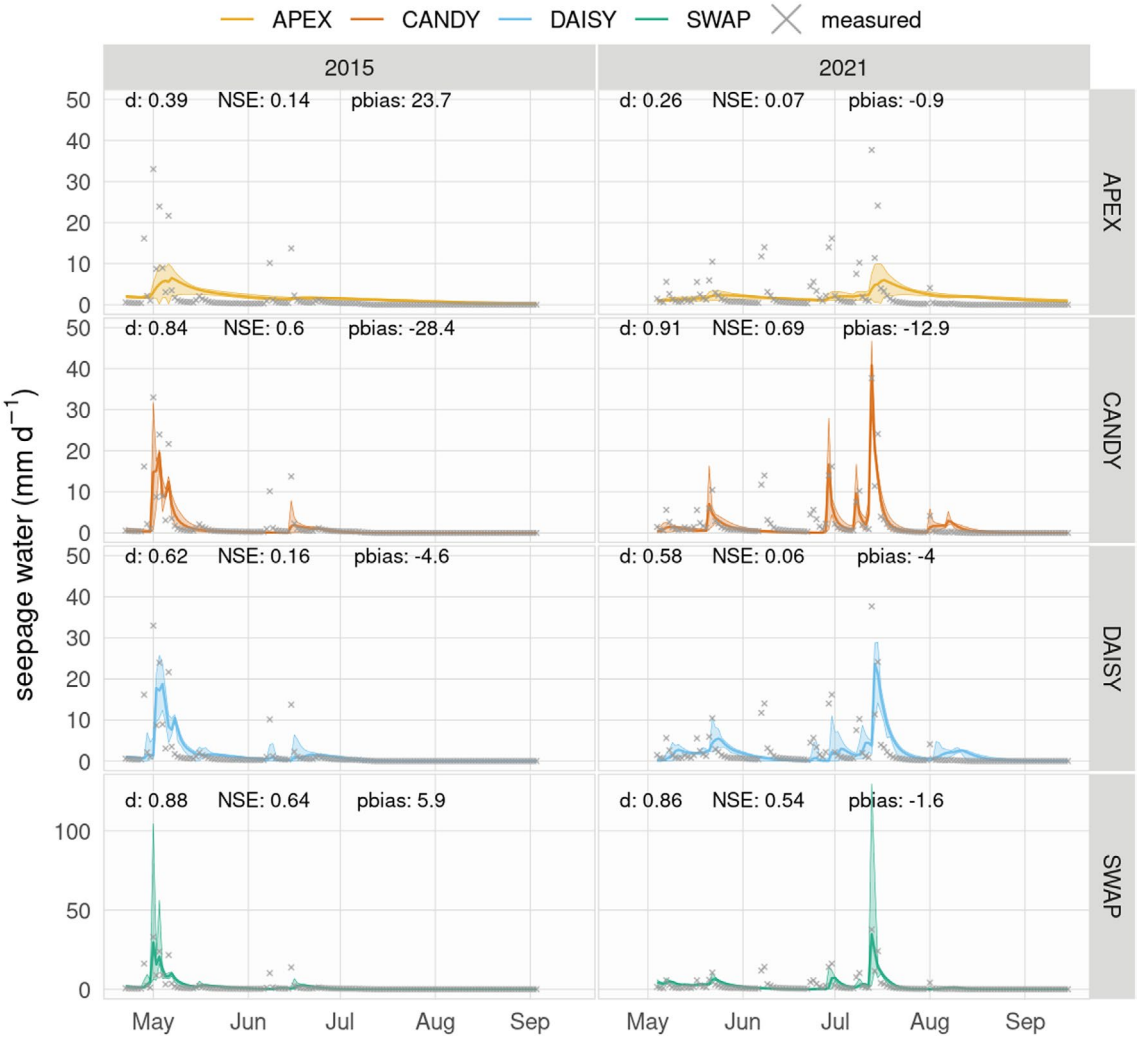

FIGURE 7 | Measured (grey crosses) and simulated daily values of seepage water during the period with silage maize in the lysimeters in the years 2015 and 2021. Full lines represent mean values among all PTFs and shading shows minimum and maximum values for each model. Metrics are calculated based on the average value from the PTF ensemble. Notice that the vertical scale is not the same for all models.

3.4 | Partitioning Variance in Simulated Outputs

In a subsequent analysis, we attributed the variance in the simulated results to the choice of the model and the choice of the PTF, as described by ANOVA. For this analysis, the simulated results from the four validated agro-hydrological models with 18 PTFs were grouped according to how models describe the soil water flux in unsaturated conditions, that is, using the Richards equation (SWAP and DAISY) or using a reservoir cascade scheme (APEX and CANDY). Note that we included the years from 2009 to 2021 in this specific analysis to obtain a broader sampling period of how the variance is propagated due to the choice of PTF compared with the model ensembles. Considering the four models and 18 PTFs, Figure 8 shows the contribution of 'model' choice, 'PTF' choice, and their interactions to the variance of the simulated soil water content, which is represented proportionally to the total range of values of soil water content per day. Regarding the full model ensemble, most of the simulated variance was attributed to the model choice. Considering DAISY and SWAP, most of the differences between simulated daily soil water content could be attributed to the PTF choice. Compared with the two Richards-based models, the two reservoir cascade models showed a much lower sensitivity to PTF choice, except for some sensitivity in the deeper soil layers of 60 and 90 cm (Figure 8). The model comparisons that included APEX showed a higher variance caused by the 'model' which can be attributed to the very different APEX model structure (Figure A17). An overview of additional combinations of model outputs is presented in Appendix A5.

To evaluate the propagation of variance in the simulated soil water content to other evaluated outputs, Figure 9 shows the variance partitioning in the simulated yearly values of aboveground biomass, transpiration, evaporation and seepage water originating from the choice of PTF and model, respectively. Using the full model ensemble (left column), the range of simulated transpiration and evaporation did not vary much between the years. The total variance in the simulated results was dominated by model structural differences in all four simulated variables, regardless of the year or the simulated output. The interaction of models versus PTF choice played only a very minor role in contributing to the variance of the four simulated

13652389, 2025, 2, Downloaded from https://bsssjournals.onlinelibrary.wiley.com/doi/10.1111/ejss.70088 by Schweizerische Akademie Der, Wiley Online Library on [27/03/2025]. See the Terms and Conditions (https://onlinelibrary.wiley.com/terms-and-conditions) on Wiley Online Library for rules of use; OA articles are governed by the applicable Creative Commons License

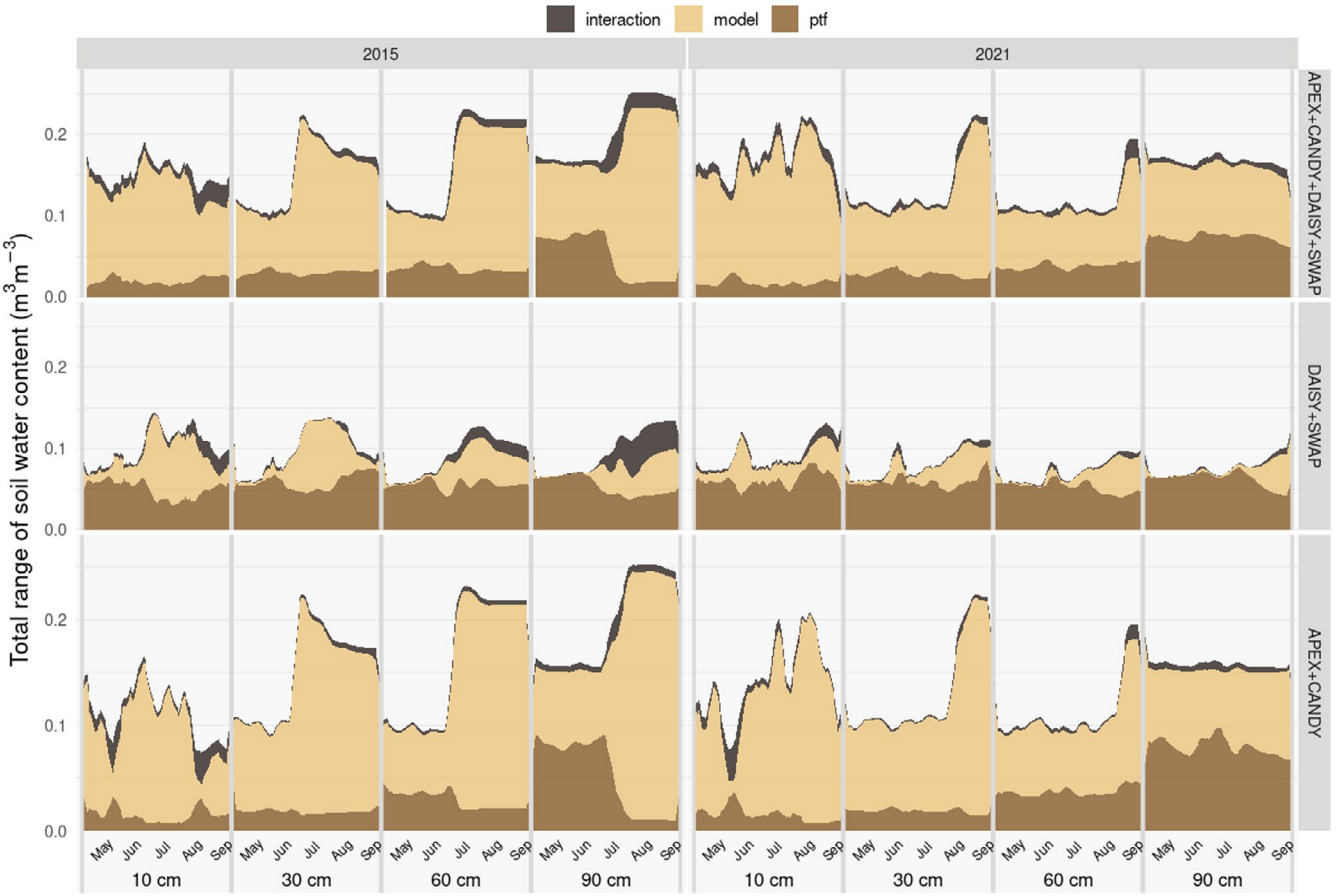

FIGURE 8 | Analysis of variance contribution of 'PTF' versus 'model' and their interactions for the simulated soil water content in selected years. The total bar size represents the range between the minimum and maximum values in all model × PTF combinations. The contribution to the variance was calculated on a daily time step during the cropping period. Plotted bars represent moving averages with a window of 10 days.

variables examined, but was higher than only the PTF contribution in most cases. For simulated aboveground biomass and seepage water, overall variance and variance sources differ substantially between the years (Figure 9). Considering only APEX and CANDY, the variance in simulated evaporation and transpiration stems almost entirely from the model choice, while PTF choice has hardly any influence on these results. Discrepancies in the descriptions of the soil hydraulic processes in CANDY and APEX play a determinant role in governing this variance in the simulations (e.g., field capacity definition, soil discretization). However, it is also evident that the variance in simulating transpiration was the lowest in both of these reservoir cascade models, indicating that they mostly agree in the simulation of transpiration.

4 | Discussion

4.1 | Agro-Hydrological Model Performance

When simulating the total aboveground biomass, AET, seepage water and soil water content, the ensemble of PTFs provided better model results than when using one unique PTF for all the simulated variables in all models. No single PTF could provide the best metric for every model and evaluated output (Figures A8–A11). This finding is supported by the study from Guber et al. (2006), who found that the error in simulating water components using PTF ensembles was on average two times smaller compared with simulation performances based on single PTFs. Similarly, Zhang et al. (2020) showed that for predicting soil water content, using an ensemble of PTFs was better than any individual PTF. When we compared the differences in model performance and examined the PTF choice, no systematic effect of PTF complexity or PTF geographic origin (i.e., EU or USA) on model performance could be identified, as also reported by Weihermüller et al. (2021).

Amongst the four models applied in this study, no single model outperformed any other for every output variable of interest. In this study, APEX simulated the aboveground biomass and AET well, but had a weaker performance in simulating the dynamics of soil water content and seepage water. For CANDY, it was the other way around, and the model performed well with respect to seepage water, AET and soil water content simulation, but underestimated the observed aboveground biomass. DAISY performed well in estimating aboveground biomass, cumulative seepage water and soil water content but did not perform as well for daily seepage water and AET. SWAP performed well on average for all simulated outputs but was very sensitive to the choice of PTFs, which indicates that very poor results can be obtained when using a single SHP parametrisation. One important remark is that the models were developed

13652389, 2025, 2, Downloaded from https://bsssjournals.onlinelibrary.wiley.com/doi/10.1111/ejss.70088 by Schweizerische Akademie Der, Wiley Online Library on [27/03/2025]. See the Terms and Conditions (https://onlinelibrary.wiley.com/terms-and-conditions) on Wiley Online Library for rules of use; OA articles are governed by the applicable Creative Commons License

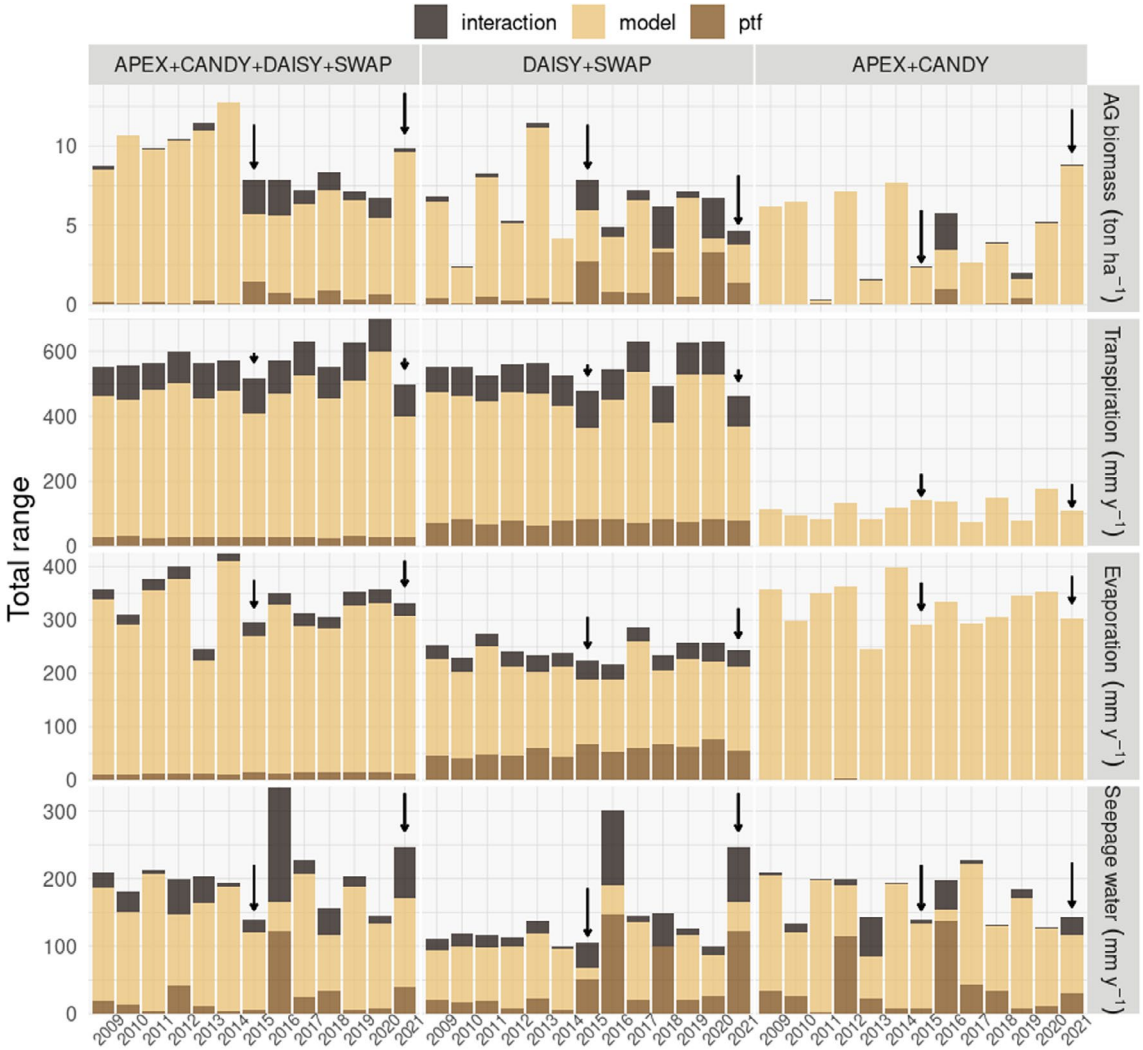

FIGURE 9 | Analysis of variance contribution of 'PTF' versus 'model' and their interactions for simulated aboveground biomass (AG biomass, Mg ha^{-1}), actual annual transpiration (mm y^{-1}), actual annual evaporation (mm y^{-1}) and annual seepage water (mm y^{-1}). The total bar size represents the range between the minimum and maximum values in all model × PTF combinations. Arrows indicate the years when silage maize was grown on the lysimeters and the models were calibrated.

to represent field conditions and, therefore, artefacts such as the oasis effect in lysimeters (Gebler et al. 2015) could not be completely captured without calibrating for AET.

When simulating the soil water content, the Richards equation-based models (DAISY and SWAP) tended to perform better than the reservoir cascade models (APEX and CANDY), particularly in deeper soil layers. This has also been reported by (Groh et al. 2020), who found the same trend in their model inter-comparison study. (Groh et al. 2020) further observed a superiority of Richards equation-based models with regard to seepage water simulations. In our study, APEX and CANDY had a lower performance in simulating cumulative seepage water (Figure A5); however, the reservoir cascade model CANDY was overall the best model for simulating the dynamics of seepage water during the growing period (Figure 7). Similar observations were also made by (Baroni et al. 2010), who noticed good predictions of soil water content even when AET and bottom flux (corresponding to seepage water in our study) were poorly predicted by both a Richards-based and a reservoir cascade model. The differences we found can be explained by the fact that different models were initially built for different purposes and therefore differ in their level of detail and complexity in representing particular process descriptions. For example, some models were developed with a prime focus on soil hydrology and incorporate only simplistic descriptions of plant growth processes (e.g., APEX, DAISY), while others have their primary focus on plant growth processes and incorporate simpler descriptions of soil water dynamics (e.g., CANDY). Such differences in levels of complexity between model components can explain the fact that the sensitivities to the PTFs differed by output and model in our study.

4.2 | Variance Attribution to Model Versus PTF Choice

Although most studies investigating the propagation of PTF uncertainty in agro-hydrological model outputs have highlighted that the choice of PTF played an important role in simulated hydrological and vegetation dynamics (Paschalis et al. 2022; Weihermüller et al. 2021; Liao et al. 2020; Baroni et al. 2010),

13652389, 2025, 2, Downloaded from https://bsssjournals.onlinelibrary.wiley.com/doi/10.1111/ejss.70088 by Schweizerische Akademie Der, Wiley Online Library on [27/03/2025]. See the Terms and Conditions (https://onlinelibrary.wiley.com/terms-and-conditions) on Wiley Online Library for rules of use; OA articles are governed by the applicable Creative Commons License

the findings of our study suggest that the uncertainties originating from model structural differences in our 4-model ensemble were overall more relevant than the uncertainties originating from the choice of PTF. Our analyses by grouping the models according to soil water model type (reservoir cascade vs. Richards equation-based) showed that the contribution from PTFs to the total variance differs substantially in relevance depending on soil water model type. Simulated variance of soil water content, seepage water and also AET were considerably affected by PTF choice within the two models integrating the Richards equation (DAISY and SWAP). However, simulation results from the two reservoir cascade models (APEX and CANDY) were less affected by the choice of PTF and were more affected by model structural differences. In addition to the limited number of input parameters required for the soil water dynamics in the reservoir cascade models, small inconsistencies, for example, in the definition of field capacity used in the model, can result in substantial differences in, for example, the soil water contents.

The effect of the agro-hydrological model structure compared to the PTF choice has not been shown by similar studies, for example, by Baroni et al. (2010) or Liao et al. (2020). Both studies concluded that the choice of PTF influences the simulated results more than the model structural differences (Baroni et al. 2010) or was at least equally important (Liao et al. 2020). These discrepancies in findings suggest that the influence of PTF choice on the simulated outputs can differ not only depending on the choice of model type (i.e., reservoir cascade vs. Richards equation) but also depending on model setups and calibration. Considerable influence of model setups on the uncertainty in the simulated outputs was, for example, observed by Folberth et al. (2019), who performed an evaluation of the performance of the global gridded crop model (GGCM EPIC) on plant stress responses, depending on soil and soil hydraulic parametrization. However, in the same study, Folberth et al. (2019) also found that structural model uncertainties outweighed any impacts of the model configuration in a larger model ensemble. Likewise, the findings from our study (with four models) in comparison to previous studies of Baroni et al. (2010) and Liao et al. (2020) (each with two models) suggest that the influence of PTF choice on the model simulations decreases with increasing size of the model ensemble.

4.3 | Structural Model Differences

In addition to different levels of model sensitivity to the choice of PTFs, model choice played a major role in determining the range of simulated outputs. As one major difference, APEX uses a default FC of 330 cm and CANDY uses a default value of 63 cm suction. Some of the differences in the simulated variables could be attributed to FC parametrization, whereas other differences are the result of the crop parameterization in the models. The lower FC in APEX was expected to lead to less plant available water compared to CANDY, which was evident in APEX particularly when the soil water content dropped below about 0.2 cm^{-3} then the soil water content decreased rapidly and led to minimum soil water contents and overall lower values (Figure 5), while CANDY captured the dynamics of the soil water content and seepage generation. The different suctions used by the two reservoir cascade models go back to older discussions regarding the pressure head at which FC should be defined (see for example Turek et al. (2020) and literature cited therein). As described by Romano and Santini (2002), FC is a process-dependent parameter that depends on the water content distribution within the soil profile and cannot be treated as a static soil property, which is a widely known drawback of the reservoir cascade models, despite chosen FC.

Even using an aligned strategy to calibrate the crop and choosing the well-established Penman–Monteith equation to calculate evapotranspiration fluxes, differences in PET and AET were observed (Figure 6). This is because parameters within the equation, such as the canopy resistance factor, were different and ideally had to be set or calibrated. The differences in how crop transpiration is modelled were shown to account for a large proportion of uncertainty in model ensembles (Cammarano et al. 2016). Likewise, Kimball et al. (2019) showed that the choice of PET estimation was the most influential factor in predicting AET between crop models. Differences in AET calculations were shown to lead to different crop parameterisations, in particular under water stress conditions (Cammarano et al. 2023). If measured AET values were available during the calibration phase, these could have been used in the calibration and would have removed one layer within the model structural differences (uncertainty). In CANDY, its relatively simple approach overestimated AET at the beginning of the growing period, which was certainly related to the comparatively early beginning of the crop growth and LAI development, as well as the approach used in the model to calculate AET (see Figures 6 and A12). Regarding water stress, the plant transpiration in SWAP was also limited by wet conditions (Figure A14), including another process that was not taken into account by the other models, so in this model, the difference between potential and actual evapotranspiration cannot be directly linked to drought.

In Figure 6, the AET simulated in mid-July in 2015 shows larger variations in SWAP compared with the other three models. This indicates that in a dry year, the choice of PTF is especially important in SWAP. It is also worth noting that the LAI in SWAP was the highest, with the most variability, of all models (Figure A12). In the wet year 2021, the AET simulated in mid-June in DAISY was higher compared with the other models. The LAI was lowest in DAISY and explains the lower plant water loss during this time. The LAI was not parametrised the same in all models, which is an additional source of model structural differences. It could be of further interest to examine whether calibrating using the LAI during the growing season leads to better model performances compared with calibrating using only the yield data. Furthermore, it is interesting to note that although the phenology in the models DAISY, SWAP and CANDY was well matched to the available phenology data, the shape of the LAI is very different between all models (see Figure A12). It is important to note that the phenology data was not obtained from the lysimeters and therefore was an additional source of uncertainty. The rooting depth dynamics also varied according to the model, adding one more layer to the model structural differences (see Figure A13). Only SWAP and CANDY presented some sensitivity to the PTFs in estimating the rooting depth, but only in SWAP was a substantial reduction observed.

13652389, 2025, 2, Downloaded from https://bsssjournals.onlinelibrary.wiley.com/doi/10.1111/ejss.70088 by Schweizerische Akademie Der, Wiley Online Library on [27/03/2025]. See the Terms and Conditions (https://onlinelibrary.wiley.com/terms-and-conditions) on Wiley Online Library for rules of use; OA articles are governed by the applicable Creative Commons License

Additionally, and as emphasised by Wallach et al. (2021), these findings highlight the importance of the parameter values selected during the calibration process, which are strongly dependent on the target variables chosen for calibrating. In this study, we applied a common approach for calibrating only the crop parameters based on aboveground biomass; we chose not to change the soil parameters. The focus of the study was on investigating uncertainties resulting from PTF choices and model choice; therefore, we did not quantify uncertainties originating from parameter choices during the calibration. Previous studies showed that model structural differences usually dominate over the uncertainty in the crop parametrisation (e.g., Tao et al. (2018), Wallach et al. (2017)). However, for future work, it may be advisable to investigate to what extent the sensitivities to PTF uncertainties differ, not only depending on model choice but also depending on crop parametrisation. This connects to the fact that the calibration procedure allowed flexibility for the models to tune their various parameters in such a way that each model was able to match the calibrated data. As a result, the crop simulated by each model had different allocations of biomass. In SWAP, less biomass was allocated to the roots, but the leaf area index was large, while DAISY allocated less to the leaves but had a bigger amount of roots (For details see appendix Figures A12 and A13). These trade-offs would have been reduced if more data were available, such as LAI over the growing season.

5 | Conclusions

In this study, we systematically evaluated the simulated outputs by four agro-hydrological models, including the variance partitioning into two different variance sources: PTF choice and model choice. To our knowledge, our study is the first to investigate the influence of PTF choice in comparison to model choice (i.e., model structural uncertainty), considering more than two models. In our four-model ensemble, the choice of PTF proved to be overall less influential than the model structural differences. Within the PTF/model ensemble, the importance of PTF choice differed depending on how the soil hydraulic properties are represented in the model (point or continuous) and output variable of interest (with water balance components being more sensitive to PTF choice than plant growth-related outputs). Since the model structure contributes to a large part of the simulated variance, it is important to carefully consider the choice of agro-hydrological model and its setup in alignment with the research objective. For all four models, the simulation of the soil water balance-related outputs averaged over all PTFs was better than when choosing any single PTF for the simulation. From these findings, we conclude that the application of PTF ensembles can be recommended for improving agro-hydrological model performance accuracy and robustness of the simulated water-balance-related outputs (i.e., soil water content and seepage water/bottom flux) – particularly, where Richards-based models are applied. However, it should be noted that model structural uncertainties are likely to outweigh variance from PTF choice in larger model ensembles. With that, the benefits of considering PTF ensembles are likely to decrease as more models are integrated into the analysis. Further work should be done to investigate this hypothesis and also to quantify to what extent the influences of PTF choice might differ depending on crop parameterisation.

Author Contributions

Maria Eliza Turek: conceptualization, methodology, software, data curation, investigation, validation, formal analysis, visualization, writing – original draft, writing – review and editing, resources. **Johannes Wilhelmus Maria Pullens:** conceptualization, methodology, software, investigation, validation, formal analysis, writing – original draft, writing – review and editing, resources. **Katharina Hildegard Elisabeth Meurer:** conceptualization, investigation, writing – original draft, validation, methodology, writing – review and editing, software, formal analysis, resources. **Edberto Moura Lima:** conceptualization, investigation, writing – original draft, writing – review and editing, methodology, validation, software, formal analysis, resources. **Bano Mehdi-Schulz:** conceptualization, investigation, writing – original draft, methodology, validation, writing – review and editing, software, formal analysis, resources. **Annelie Holzkämper:** conceptualization, investigation, funding acquisition, writing – original draft, methodology, validation, writing – review and editing, formal analysis, project administration, supervision, resources.

Acknowledgements

This project was developed in the framework SoilX-EJP SOIL projects. SoilX is part of the European Joint Program for SOIL Towards climate-smart sustainable management of agricultural soils (EJP SOIL) funded by the European Union Horizon 2020 research and innovation programme (Grant Agreement N° 862695). The authors further acknowledge the helpful comments of the two reviewers.

Conflicts of Interest

The authors declare no conflicts of interest.

Data Availability Statement

Model setup and output datasets can be found in \href{https://doi.org/10.5281/zenodo.13947787}{Zenodo}. Data processing scripts are stored in \href{https://gitlab.com/gsf8705208/proj_uncertainty_ptf_soilx}{GitLab}.

References

Abrahamsen, P., and S. Hansen. 2000. "Daisy: An Open Soil-Crop-Atmosphere System Model." *Environmental Modelling & Software* 15: 313–330. https://www.sciencedirect.com/science/article/pii/S1364815200000037.

Agroscope. 2024. "Standortcharakterisierung." https://www.agroscope.admin.ch/agroscope/de/home/themen/umwelt-ressourcen/monitoring-analytik/referenzmethoden/standortcharakterisierung.html.

Allen, R. G., L. S. Pereira, D. Raes, et al. 1998. *Crop Evapotranspiration-Guidelines for Computing Crop Water Requirements-Fao Irrigation and Drainage Paper 56*. Vol. 300, D05109. Fao.

Baffaut, C., N. O. Nelson, J. A. Lory, et al. 2017. "Multisite Evaluation of Apex for Water Quality: I. Best Professional Judgment Parameterization." *Journal of Environmental Quality* 46: 1323–1331.

Baroni, G., A. Facchi, C. Gandolfi, B. Ortuani, D. Horeschi, and J. C. Dam. 2010. "Uncertainty in the Determination of Soil Hydraulic Parameters and Its Influence on the Performance of Two Hydrological Models of Different Complexity." *Hydrology and Earth System Sciences* 14: 251–270. https://hess.copernicus.org/articles/14/251/2010/.

Bartholomeus, R. P., J.-P. M. Witte, P. M. Bodegom, J. C. Dam, and R. Aerts. 2008. "Critical Soil Conditions for Oxygen Stress to Plant Roots: Substituting the Feddes-Function by a Process-Based Model." *Journal of Hydrology* 360: 147–165. https://www.sciencedirect.com/science/article/pii/S0022169408003752.

13652389, 2025, 2, Downloaded from https://bsssjournals.onlinelibrary.wiley.com/doi/10.1111/ejss.70088 by Schweizerische Akademie Der, Wiley Online Library on [27/03/2025]. See the Terms and Conditions (https://onlinelibrary.wiley.com/terms-and-conditions) on Wiley Online Library for rules of use; OA articles are governed by the applicable Creative Commons License

Baux, A., J. Hiltbrunner, J.-F. Collaud, L. Deladoey, and U. Buchmann. 2010. "Silomais hauptversuch 2009–2010. Tech. rep., Hrsg. Agroscope, Reckenholz." http://www.agroscope.ch/mais/03274/index.html?lang=de.

Cammarano, D., J. Pullens, and P. Martre. 2023. "Modeling Climate Change Impacts on Crop Growth and Yield Formation." In *Modelling Climate Change Impacts on Agricultural Systems*, edited by C. Nendel, 156–187. Burleigh Dodds Science Publishing Limited.

Cammarano, D., R. P. Rötter, S. Asseng, et al. 2016. "Uncertainty of Wheat Water Use: Simulated Patterns and Sensitivity to Temperature and CO_2." *Field Crops Research* 198: 80–92. https://www.sciencedirect.com/science/article/pii/S0378429016302726.

Deng, H., M. Ye, M. G. Schaap, and R. Khaleel. 2009. "Quantification of Uncertainty in Pedotransfer Function-Based Parameter Estimation for Unsaturated Flow Modeling." *Water Resources Research* 45: W04409.

Ding, X., and A. El-Zein. 2024. "Predicting Soil Water Retention Curves Using Machine Learning: A Study of Model Architecture and Input Variables." *Engineering Applications of Artificial Intelligence* 133: 108122. https://www-sciencedirect-com.agros.swissconsortium.ch/science/article/pii/S095219762400280X.

Doro, L., C. Jones, J. R. Williams, et al. 2017. "The Variable Saturation Hydraulic Conductivity Method for Improving Soil Water Content Simulation in Epic and Apex Models." *Vadose Zone Journal* 16: 1–14. https://doi.org/10.2136/vzj2017.06.0125.

Feddes, R. A., P. J. Kowalik, and H. Zaradny. 1978. "Simulation of Field Water Use and Crop Yield. Simulation Monographs. Pudoc Outside the U.S.A., Canada and Latin America." https://edepot.wur.nl/168026.

Folberth, C., J. Elliott, C. Müller, et al. 2019. "Parameterization-Induced Uncertainties and Impacts of Crop Management Harmonization in a Global Gridded Crop Model Ensemble." *PLoS One* 14: 1–36. https://doi.org/10.1371/journal.pone.0221862.

Franko, U., B. Oelschlägel, and S. Schenk. 1995. "Simulation of Temperature-, Water- and Nitrogen Dynamics Using the Model Candy." *Ecological Modelling* 81: 213–222.

Franko, U., B. Oelschlägel, S. Schenk, et al. 2024. "CANDY 22 Manual III." http://www.frug.info/candy_main.php. Software available for download at. www.frug.info/candy_main.php.

Gardner, W. 1958. "Some Steady State Solutions of the Unsaturated Moisture Flow Equation With Application to Evaporation From a Water Table." *Soil Science* 85: 228–232.

Gassman, P. W., J. R. Williams, X. Wang, et al. 2009. "The Agricultural Policy Environmental Extender (APEX) Model: An Emerging Tool for Landscape and Watershed Environmental Analyses. *Technical Report 41*, Center for Agricultural and Rural Development, Ames, IA, USA."

Gebler, S., H.-J. Hendricks Franssen, T. Pütz, H. Post, M. Schmidt, and H. Vereecken. 2015. "Actual Evapotranspiration and Precipitation Measured by Lysimeters: A Comparison With Eddy Covariance and Tipping Bucket." *Hydrology and Earth System Sciences* 19: 2145–2161. https://hess.copernicus.org/articles/19/2145/2015/.

Genuchten, M. T. 1980. "A Closed-Form Equation for Predicting the Hydraulic Conductivity of Unsaturated Soils." *Soil Science Society of America Journal* 44: 892–898. https://doi.org/10.2136/sssaj1980.03615995004400050002x.

Groh, J., E. Diamantopoulos, X. Duan, et al. 2020. "Crop Growth and Soil Water Fluxes at Erosion-Affected Arable Sites: Using Weighing Lysimeter Data for Model Intercomparison." *Vadose Zone Journal* 19: e20058. https://doi.org/10.1002/vzj2.20058.

Guber, A. K., Y. A. Pachepsky, M. T. Genuchten, et al. 2006. "Field-Scale Water Flow Simulations Using Ensembles of Pedotransfer Functions for Soil Water Retention." *Vadose Zone Journal* 5: 234–247. https://doi.org/10.2136/vzj2005.0111.

Hanks, R. J. 1983. "Yield and Water-Use Relationships: An Overview." In *Limitations to Efficient Water Use in Crop Production*, edited by H. M. Taylor, W. R. Jordan, and T. R. Sinclair, 393–411. American Society of Agronomy, Crop Science Society of America, Soil Science Society of America.

Hansen, S. 1984. "Estimation of Potential and Actual Evapotranspiration: Paper Presented at the Nordic Hydrological Conference (Nyborg, Denmark, August – 1984)." *Hydrology Research* 15: 205–212. https://doi.org/10.2166/nh.1984.0017.

Hansen, S., H. E. Jensen, N. E. Nielsen, and H. Svendsen. 1991. "Simulation of Nitrogen Dynamics and Biomass Production in Winter Wheat Using the Danish Simulation Model Daisy." *Fertilizer Research* 27: 245–259. https://doi.org/10.1007/bf01051131.

Hiltbrunner, J., M. Benincore, T. Huber, and P. Pignon. 2023. "Resultate der hauptversuche silomais 2022–2023. Tech. Rep. 508, Agroscope Transfer." http://www.agroscope.ch/mais/03274/index.html?lang=de.

Hiltbrunner, J., M. Bertossa, U. Buchmann, et al. 2014. "Silomais hauptversuch 2013–2014. Tech. rep., Hrsg. Agroscope, Changins." http://www.agroscope.ch/mais/03274/index.html?lang=de.

Hiltbrunner, J., M. Bertossa, U. Buchmann, et al. 2015. "Silomais hauptversuch 2014–2015: Resultatheft. Tech. rep., Hrsg. Agroscope, Reckenholz." http://www.agroscope.ch/mais/03274/index.html?lang=de.

Hiltbrunner, J., U. Buchmann, and P. Pignon. 2016. "Resultate der hauptversuche silomais 2015–2016. Tech. Rep. 148, Agroscope Transfer." http://www.agroscope.ch/mais/03274/index.html?lang=de.

Hiltbrunner, J., U. Buchmann, and P. Pignon. 2017. "Resultate der hauptversuche silomais 2016–2017. Tech. Rep. 206, Agroscope Transfer." http://www.agroscope.ch/mais/03274/index.html?lang=de.

Hiltbrunner, J., U. Buchmann, and P. Pignon. 2018. "Resultate der hauptversuche silomais 2017–2018. Tech. Rep. *254*, Agroscope Transfer." http://www.agroscope.ch/mais/03274/index.html?lang=de.

Hiltbrunner, J., U. Buchmann, and P. Pignon. 2019. "Resultate der hauptversuche silomais 2018–2019. Tech. Rep. 301, Agroscope Transfer." http://www.agroscope.ch/mais/03274/index.html?lang=de.

Hiltbrunner, J., T. Huber, and P. Pignon. 2020. "Resultate der hauptversuche silomais 2019–2020. Tech. Rep. 364, Agroscope Transfer." http://www.agroscope.ch/mais/03274/index.html?lang=de.

Hiltbrunner, J., T. Huber, and P. Pignon. 2021. "Resultate der hauptversuche silomais 2020–2021. Tech. Rep. 416, Agroscope Transfer." http://www.agroscope.ch/mais/03274/index.html?lang=de.

Hiltbrunner, J., T. Huber, and P. Pignon. 2022. "Resultate der hauptversuche silomais 2021–2022. Tech. Rep. 457, Agroscope Transfer." http://www.agroscope.ch/mais/03274/index.html?lang=de.

Huang, Y., Y. Yu, W. Zhang, et al. 2009. "Agro-c: A Biogeophysical Model for Simulating the Carbon Budget of Agroecosystems." *Agricultural and Forest Meteorology* 149: 106–129. https://www.sciencedirect.com/science/article/pii/S0168192308002062.

Izaurralde, R. C., J. R. Williams, W. B. McGill, N. J. Rosenberg, and M. C. Q. Jakas. 2006. "Simulating Soil c Dynamics With Epic: Model Description and Testing Against Long-Term Data." *Ecological Modelling* 192: 362–384.

Jones, C. D., A. D. Reddy, J. Jeong, et al. 2021. "Improved Hydrological Modeling With Apex and Epic: Model Description, Testing, and Assessment of Bioenergy Producing Landscape Scenarios." *Environmental Modelling & Software* 143: 105111.

Kimball, B. A., K. J. Boote, J. L. Hatfield, et al. 2019. "Simulation of Maize Evapotranspiration: An Inter-Comparison Among 29 Maize Models." *Agricultural and Forest Meteorology* 271: 264–284. https://www.sciencedirect.com/science/article/pii/S0168192319300966.

Koitzsch, R., and R. Günther. 1990. "Modell zur ganzjährigen simulation der verdunstung und der bodenfeuchte landwirtschaftlicher

13652389, 2025, 2, Downloaded from https://bsssjournals.onlinelibrary.wiley.com/doi/10.1111/ejss.70088 by Schweizerische Akademie Der, Wiley Online Library on [27/03/2025]. See the Terms and Conditions (https://onlinelibrary.wiley.com/terms-and-conditions) on Wiley Online Library for rules of use; OA articles are governed by the applicable Creative Commons License

nutzflächen mit und ohne bewuchs." *Archiv für Acker Und Pflanzenbau Und Bodenkunde = Archives of Agronomy and Soil Science* 34: 803–810.

Kroes, J. G., J. G. Wesseling, and J. C. Dam. 2000. "Integrated Modelling of the Soil–Water–Atmosphere–Plant System Using the Model Swap 20 an Overview of Theory and an Application." *Hydrological Processes* 14: 1993–2002. https://doi.org/10.1002/1099-1085%2820000815/30%2914%3A11/12%3C1993%3A%3AAID-HYP50%3E3.0.CO%3B2-%23.

Kroes, J. G., J. C. Dam, R. P. Bartholomeus, et al. 2017. "SWAP 4 – Theory Including User Manual." In *Tech. Rep.* Wageningen University and Research. https://www.swap.alterra.nl/Documents/Kroes_etal_2017_SWAP_version_4_ESG_Report_2780.pdf.

Li, L., B. Wang, P. Feng, et al. 2023. "The Optimization of Model Ensemble Composition and Size Can Enhance the Robustness of Crop Yield Projections." *Communications Earth & Environment* 4, no. 1: 362. https://doi.org/10.1038/s43247-023-01016-9.

Liao, K., X. Lai, Z. Zhou, Y. Liu, and Q. Zhu. 2020. "Uncertainty Analysis and Ensemble Bias-Correction Method for Predicting Nitrate Leaching in Tea Garden Soils." *Agricultural Water Management* 237: 106182. https://www-sciencedirect-com.agros.swissconsortium.ch/science/article/pii/S0378377420301098.

Loosvelt, L., V. R. N. Pauwels, W. M. Cornelis, G. J. M. Lannoy, and N. E. C. Verhoest. 2011. "Impact of Soil Hydraulic Parameter Uncertainty on Soil Moisture Modeling." *Water Resources Research* 47: W03505.

Looy, K., J. Bouma, M. Herbst, et al. 2017. "Pedotransfer Functions in Earth System Science: Challenges and Perspectives." *Reviews of Geophysics* 55: 1199–1256.

Mason, R., J. Gorres, J. W. Faulkner, L. Doro, and S. C. Merrill. 2020. "Calibrating the Apex Model for Simulations of Environmental and Agronomic Outcomes on Dairy Farms in the Northeast U.S.: A Step-By-Step Example." *Applied Engineering in Agriculture* 36: 281–301.

Meier, U., H. Bleiholder, E. Weber, et al. 2001. "Bbch Monograph, Growth Stages of Mono and Dicotyledonous Plants. Tech. rep., Federal Biological Research Centre for Agriculture and Forestry, Germany." https://www.politicheagricole.it/flex/AppData/WebLive/Agrometeo/MIEPFY800/BBCHengl2001.pdf.

Mualem, Y. 1976. "A New Model for Predicting the Hydraulic Conductivity of Unsaturated Porous Media." *Water Resources Research* 12: 513–522. https://doi.org/10.1029/WR012i003p00513.

Mullen, K., D. Ardia, D. Gil, D. Windover, and J. Cline. 2011. "DEoptim: An R Package for Global Optimization by Differential Evolution." *Journal of Statistical Software* 40: 1–26. https://cran.r-project.org/package=DEoptim.

Nash, J. E., and J. V. Sutcliffe. 1970. "River Flow Forecasting Through Conceptual Models Part i — A Discussion of Principles." *Journal of Hydrology* 10: 282–290. http://linkinghub.elsevier.com/retrieve/pii/0022169470902556.

Nasta, P., B. Szabó, and N. Romano. 2021. "Evaluation of Pedotransfer Functions for Predicting Soil Hydraulic Properties: A Voyage From Regional to Field Scales Across Europe." *Journal of Hydrology: Regional Studies* 37: 100903. https://www.sciencedirect.com/science/article/pii/S2214581821001324.

Oberholzer, S., V. Prasuhn, and A. Hund. 2017. "Crop Water Use Under Swiss Pedoclimatic Conditions – Evaluation of Lysimeter Data Covering a Seven-Year Period." *Field Crops Research* 211: 48–65. https://www.sciencedirect.com/science/article/pii/S0378429017302125.

Paschalis, A., S. Bonetti, Y. Guo, and S. Fatichi. 2022. "On the Uncertainty Induced by Pedotransfer Functions in Terrestrial Biosphere Modeling." *Water Resources Research* 58: e2021WR031871. https://doi.org/10.1029/2021WR031871.

Prasuhn, V., C. Humphrys, and E. Spiess. 2016. "Seventy-Two Lysimeters for Measuring Water Flows and Nitrate Leaching Under Arable Land." In *NAS International Workshop on Applying the Lysimeter Systems to Water and Nutrient Dynamics*, 1–24. National Institute of Agricultural Sciences.

Puy, A., S. L. Piano, A. Saltelli, and S. A. Levin. 2022. "Sensobol: An R Package to Compute Variance-Based Sensitivity Indices." *Journal of Statistical Software* 102: 1–37. https://github.com/arnaldpuy/sensobol.

R Core Team. 2024. *R: A Language and Environment for Statistical Computing*. R Foundation for Statistical Computing. https://www.R-project.org/.

Ritchie, J. T. 1972. "A Model for Predicting Evaporation From a Row Crop With Incomplete Cover." *Water Resources Research* 8: 1204–1213. https://doi.org/10.1029/WR008i005p01204.

Romano, N., and A. Santini. 2002. "Water Retention and Storage, Field Methods." In *SSSA (Part 4. Physical Methods), Methods of Soil Analysis*, 723–729. SSSA.

Schaap, M. G., F. J. Leij, and M. T. Genuchten. 2001. "Rosetta: A Computer Program for Estimating Soil Hydraulic Parameters With Hierarchical Pedotransfer Functions." *Journal of Hydrology* 251: 163–176. https://www.sciencedirect.com/science/article/pii/S0022169401004668.

Schaap, M. G., A. Nemes, and M. T. Genuchten. 2004. "Comparison of Models for Indirect Estimation of Water Retention and Available Water in Surface Soils." *Vadose Zone Journal* 3: 1455–1463. https://doi.org/10.2136/vzj2004.1455.

Stenemo, F., and N. Jarvis. 2007. "Accounting for Uncertainty in Pedotransfer Functions in Vulnerability Assessments of Pesticide Leaching to Groundwater." *Pest Management Science* 63: 867–875. https://doi.org/10.1002/ps.1415.

Szabó, B., M. Weynants, and T. K. D. Weber. 2021. "Updated European Hydraulic Pedotransfer Functions With Communicated Uncertainties in the Predicted Variables (euptfv2)." *Geoscientific Model Development* 14: 151–175. https://gmd.copernicus.org/articles/14/151/2021/.

Tao, F., R. P. Rötter, T. Palosuo, et al. 2018. "Contribution of Crop Model Structure, Parameters and Climate Projections to Uncertainty in Climate Change Impact Assessments." *Global Change Biology* 24: 1291–1307. https://doi.org/10.1111/gcb.14019.

Turek, M. E., Q. Jong van Lier, and R. A. Armindo. 2020. "Estimation and Mapping of Field Capacity in Brazilian Soils." *Geoderma* 376: 114557. https://www.sciencedirect.com/science/article/pii/S0016706120301300.

Wallach, D., S. P. Nissanka, A. S. Karunaratne, et al. 2017. "Accounting for Both Parameter and Model Structure Uncertainty in Crop Model Predictions of Phenology: A Case Study on Rice." *European Journal of Agronomy* 88: 53–62. https://www.sciencedirect.com/science/article/pii/S1161030116301022.

Wallach, D., T. Palosuo, P. Thorburn, et al. 2021. "The Chaos in Calibrating Crop Models: Lessons Learned From a Multi-Model Calibration Exercise." *Environmental Modelling & Software* 145: 105206. https://www.sciencedirect.com/science/article/pii/S1364815221002486.

Wang, X., P. Tuppad, and J. Williams. 2011. *Modelling Agricultural Management Systems With APEX*. CAB International.

Weber, T. K. D., L. Weihermüller, A. Nemes, et al. 2024. "Hydro-Pedotransfer Functions: A Roadmap for Future Development." *Hydrology and Earth System Sciences* 28: 3391–3433. https://hess.copernicus.org/articles/28/3391/2024/.

Weihermüller, L., P. Lehmann, M. Herbst, et al. 2021. "Choice of Pedotransfer Functions Matters When Simulating Soil Water Balance Fluxes." *Journal of Advances in Modeling Earth Systems* 13: e2020MS002404. https://doi.org/10.1029/2020MS002404.

Weynants, M., H. Vereecken, and M. Javaux. 2009. "Revisiting Vereecken Pedotransfer Functions: Introducing a Closed-Form Hydraulic Model." *Vadose Zone Journal* 8: 86–95. https://doi.org/10.2136/vzj2008.0062.

13652389, 2025, 2, Downloaded from https://bsssjournals.onlinelibrary.wiley.com/doi/10.1111/ejss.70088 by Schweizerische Akademie Der, Wiley Online Library on [27/03/2025]. See the Terms and Conditions (https://onlinelibrary.wiley.com/terms-and-conditions) on Wiley Online Library for rules of use; OA articles are governed by the applicable Creative Commons License

Willmott, C. J. 1981. "On the Validation of Models." *Physical Geography* 2: 184–194. https://doi.org/10.1080/02723646.1981.10642213.

Wit, A., H. Boogaard, D. Fumagalli, et al. 2019. "25 Years of the Wofost Cropping Systems Model." *Agricultural Systems* 168: 154–167. https://www.sciencedirect.com/science/article/pii/S0308521X17310107.

Wösten, J., A. Lilly, A. Nemes, and C. Bas. 1999. "Development and Use of a Database of Hydraulic Properties of European Soils." *Geoderma* 90: 169–185. https://www.sciencedirect.com/science/article/pii/S0016706198001323.

Zambrano-Bigiarini, M. 2024. "Hydrogof: Goodness-Of-Fit Functions for Comparison of Simulated and Observed Hydrological Time Series." https://cran.r-project.org/package=hydroGOF.

Zhang, Y., and M. G. Schaap. 2017. "Weighted Recalibration of the Rosetta Pedotransfer Model With Improved Estimates of Hydraulic Parameter Distributions and Summary Statistics (rosetta3)." *Journal of Hydrology* 547: 39–53. https://www.sciencedirect.com/science/article/pii/S0022169417300057.

Zhang, Y., M. G. Schaap, and Z. Wei. 2020. "Development of Hierarchical Ensemble Model and Estimates of Soil Water Retention With Global Coverage." *Geophysical Research Letters* 47: e2020GL088819. https://agupubs.onlinelibrary.wiley.com/doi/abs/10.1029/2020GL088819.

Supporting Information

Additional supporting information can be found online in the Supporting Information section.

13652389, 2025, 2, Downloaded from https://bsssjournals.onlinelibrary.wiley.com/doi/10.1111/ejss.70088 by Schweizerische Akademie Der, Wiley Online Library on [27/03/2025]. See the Terms and Conditions (https://onlinelibrary.wiley.com/terms-and-conditions) on Wiley Online Library for rules of use; OA articles are governed by the applicable Creative Commons License